Progress in Fractional Differentiation and Applications
An International Journal

http://dx.doi.org/10.18576/pfda/120208

Bifurcation Analysis and Vaccination Strategies in Toxoplasma Gondii Dynamics Modeling for the Cat Population

Muhammad Farman[1,2,*], *Aqeel Ahmad*[1,3], *Muhammad Sohaid*[3], *Evren Hincal*[1,4], *Aseel Smerat*[5,6], *Heba Elhaddad*[7] *and Mohamed Hafez*[8,9]

[1] Department of Mathematics, Mathematics Research Center, Near East University, 99138, Turkey
[2] Department of Biostatistics and Medical Informatics, Faculty of Medicine, Karadeniz Technical University, Trabzon, Turkey
[3] Department of Mathematics, Ghazi University D G Khan 32200, Pakistan
[4] Research Center of Applied Mathematics, Khazar University, Baku, Azerbaijan
[5] Faculty of Educational Sciences, Al-Ahliyya Amman University, Amman 19328, Jordan
[6] Department of Biosciences, Saveetha School of Engineering, Saveetha Institute of Medical and Technical Sciences, Chennai, India
[7] Department of Mechanical and Industrial Engineering, College of Engineering and Computing, Liwa University, Abu-Dhabi, United Arab Emirates
[8] Faculty of Engineering and Quantity Surviving, INTI International University Colleges, Nilai, Malaysia
[9] Faculty of Mangement, Shinawatra, Pathum Thani, Thailand

Received: 2 Jan. 2026, Revised: 18 Feb. 2026, Accepted: 20 Mar. 2026
Published online: 1 Apr. 2026

Abstract: This research introduces a new fractional-order mathematical framework to explore the spread dynamics of Toxoplasma gondii between the cat population and the environment, considering the combined effects of vaccination and sanitation. To reflect the memory-dependent and hereditary nature of biological interactions, the traditional integer-order system is reformulated through the Atangana-Baleanu-Caputo (ABC) fractional derivative. A qualitative analysis of the system establishes the conditions for the validations of newly developed model including the quantitative analysis on disease-free equilibrium for study state. Furthermore, bifurcation analysis demonstrates that the system can exhibit both forward and backward bifurcations, governed by factors such as vaccination intensity, sanitation efficacy, and fractional order values. These bifurcations indicate the possible coexistence of multiple equilibrium states and the emergence of complex transitional dynamics in disease transmission. Utilizing the ABC operator for possible solutions of the fractional order model that allows the model to capture infection persistence for control strategies more realistically. Simulation outcomes reveal that decreasing fractional orders enhances memory effects, resulting in slower but more persistent infection patterns. Overall, applying the ABC fractional modeling approach provides deeper insight into the nonlinear, memory-driven, and bifurcating behavior of T. gondii transmission and supports the development of robust, long-term control measures within cat populations.

Keywords: Human health; Toxoplasma gondii; Communicable disease; Bifurcation analysis; Qualitative analysis; Numerical simulation.

2010 Mathematics Subject Classification. Primary 26A33, 35A20; Secondary 33B15.

1 Introduction

A protozoan called Toxoplasma gondii infiltrates and parasitically lives within both humans and animals. The sole definitive hosts are Felidae (cats), with several other species acting as intermediate carriers [1]. Humans who suffer from congenital infections or compromised immune systems may face serious and perhaps fatal outcomes [2]. On the other hand, moderate symptoms, such as influenza-like symptoms or ocular inflammation (chorioretinitis), are typically seen in adults with healthy immune systems [3]. However, there have also been reported cases of severe acute toxoplasmosis in apparently healthy individuals [4]. Additionally, scientists have hypothesized that T. gondii infection may contribute to

* Corresponding author e-mail: aqeelahmad.740@gmail.com

the development of neurological disorders and immunological diseases [5]. It has been demonstrated that a strain's genetic composition affects the severity of the illness [6]. One of the most significant food borne pathogens is this parasite [7]. It is estimated that approximately 40 million people are infected in the United States alone. Some communities worldwide have a prevalence of above 60%, and areas with warm, humid conditions and low altitudes tend to have higher infection rates [8]. For example, T. gondii has more genetic diversity in South American tropical regions. Congenital infections account for approximately 32 per cent of the global toxoplasmosis burden [9]. With an estimated 190,000 congenital cases annually (about 1.5 per 1,000 live births), the condition is found in every nation [10]. However, the number of acquired infections remains unknown. According to estimates, there are 58 occurrences of congenital toxoplasmosis for every 100,000 persons in the United States [11]. Toxoplasmosis ranks third among food-related illnesses in terms of associated yearly health costs, with 10,964 quality-adjusted life years lost, and second in terms of associated economic burden, with an estimated USD 2.9 billion. Many nations with inadequate resources, including those in South America, have reported similarly high expenses [12].

Ingestion of sporulated oocysts, ingestion of live tissue cysts in undercooked meat, or congenital transmission from mother to fetus are the three ways that T. gondii can spread. It has been estimated that there are around 1.2 million congenital cases worldwide [13]. A large percentage of human illnesses are caused by contaminated fruits and vegetables that contain oocysts, frequently more than meat that contains bradyzoite cysts. Oocysts released by cats into the environment are a significant factor, and eating raw or improperly prepared meat can infect humans [14]. According to research, a single cat may shed up to 20 million oocysts per day, and cat faeces can contain up to 2.5×106 oocysts per gram [15]. It is challenging to control toxoplasmosis by focusing on definitive hosts [16]. Because they mainly deal with acute or reactivated instances, current health measures are limited, which emphasizes the need for more comprehensive intervention techniques. While congenital transmission may result in defects in progeny, infected animals frequently show no symptoms [17]. Different species have different known effects of T. gondii in mammals [18]. Infections have consequences for public health, financial losses, and animal health [19]. Toxoplasmosis dynamics have been examined in several previous investigations [20]. The study of disease propagation under various conditions has extensively utilized mathematical modelling using ABC techniques. Few studies have specifically examined cat-human transmission while considering demographic differences [21]. To better capture the dynamics, more complex frameworks have incorporated other hosts and factors [22]. The effects of immunization in pig and cat populations have also been studied [23]. Additionally, within-host models have been developed to characterize the dynamics of parasites within afflicted individuals [24].

This study examines the consequences of adding two distinct time delays to a mathematical model that depicts the dynamics of toxoplasmosis transmission while taking environmental oocysts and cat populations into account. Although mathematical constructs can never entirely replicate real-world processes, adding two delays to the model gives it a more realistic feel. The first period describes the latency phase in cats following infection, whereas the second period describes the time required for discharged oocysts to reach an infectious state. In particular, a vulnerable cat must go through an incubation period after consuming an oocyst before it can begin to release more. In cats, this time frame is equivalent to the latency phase. We create a nonlinear system of delay differential equations to describe these processes. The inability of cats to eliminate oocysts immediately after infection is a crucial characteristic. Since oocysts are the primary cause of T. gondii persistence, it is imperative to include them [25]. Our model builds on previous frameworks, such as, which lacked temporal delays, and recognizes direct transmission to cats through contact with infected oocysts. According to empirical research, oocyst shedding happens three to thirty days following tissue cyst consumption [26]. Since cats play a key role in parasite multiplication and, consequently, in the spread of toxoplasmosis, the feline host must be included [27]. Domestic cats and intermediate hosts are among the many factors that must be addressed for disease control to be effective. Types I, II and III are the three main genotypes of T. gondii. These types predominates in congenital infections in the US and Europe. The present model is applicable if we assume an average behaviour across all kinds, even when their levels of virulence vary. However, a more complex framework would be needed to account for genotype-specific pathogenicity. When examining the kinetics and behaviour of infectious illnesses, fractional-order models outperform traditional integer models [28]. Recently, many researchers have shown that fractional-order differential equations are valuable mathematical tools for modeling a wide range of phenomena, as they capture the memory and hereditary properties of various materials and processes. These equations are applied in several fields, including biology, medicine, fluid mechanics, and materials science [29]. Some epidemic models based on fractional-order techniques are presented in [30,31], while advanced applications of novel fractional operators to real-life problems are investigated in [32,33], contributing significantly to scientific research. Various authors have also studied different operators, particularly non-local operators and partial differential equations (PDEs) [34], which play a crucial role in modeling complex systems in biology and finance. Understanding these operators is essential for analyzing and solving problems in such fields [35].

With a generalized incidence rate, we developed the SVI_1I_2R model and suggested a novel method to efficiently manage it, concentrating on both the protected and infected cat groups to improve reader understanding. Key terms, background data, and the introduction are presented in Section 1. Section 2 describes the new mathematical model that was created in

accordance with the goals of the study. The Mathematical Model with the Fractional ABC Operator is presented in Section 3 for validation. The Flip Bifurcation study, which was carried out using MATLAB to offer a full physical understanding, and the equilibrium locations are covered in Section 4. we examines the numerical approach in section 5. While the physical interpretation and conclusion are presented in Sections 6 and 7.

1.1 Key Definitions

Definition 1.1. Suppose $0 < \iota \leq 1$ and $\chi(t) \in M^1[0,T]$. An explanation of the ABC-type fractional differentiation [36] of order μ is provided as

$$ {}_0^{ABC}D_t^{\mu}(\chi(t)) = \frac{\mathbb{G}(\mu)}{1-\mu}\int_0^{\mathrm{t}} F_{\mu}\left(-\frac{\mu}{1-\mu}(\mathrm{t}-\delta)^{\mu}\right)\frac{d}{d\delta}\chi(\delta)\,d\delta, \tag{1}$$

While $\mathbb{G}(\mu)$ denotes a scaling function fulfilling $\mathbb{G}(0) = \mathbb{G}(1) = 1$, $F_{\mu}(x)$ represents the single-parameter Mittag-Leffler function supplied by $\mathbb{G}(\mu)$.

$$F_{\mu}(z) = \sum_{l=0}^{\infty}\frac{z^l}{\Gamma(\mu l+1)}, \tag{2}$$

where the Gamma function is represented by $\Gamma(\cdot)$ and $\aleph(\mu) > 0$ holds.

2 Mathematical Model

The mathematical modeling of Toxoplasma gondii examines its transmission dynamics between cats and the environment. The framework integrates vaccination to lower infection rates in cats and sanitation measures to accelerate oocyst removal. It offers valuable insights into managing the parasite's spread and persistence under various control strategies. In this model, objectives are to divide the infected class in two classes primary and secondary infected classes. It is observed if we identify the non symptomatic class by early identification measures then it be controlled efficiently and symptomatic infected will automatically reduces. Also we want to observe the vaccination effects with combine effects of early interstratifications. For the said objectives, this model incorporates the number of susceptible, vaccinated, primary infected, secondary infected, and recovered to better capture the dynamics and management of the T. gondii Dynamics in Cats Under Vaccination and Sanitation. The description of the variables given in table 1 and parameters are given below in table 2 with the parameter values in the desired domain to achieve the objectives, then this model can be implemented on the real data except the uncertain situation.

Description of Variables

Variable	Description
$S(t)$	Susceptible Cats.
$V(t)$	Vaccinated Cats.
$I_1(t)$	Primary stage infected cats.
$I_2(t)$	Secondary stage infected cats.
$R(t)$	Recovered cats.

Table 1: Description of the Variable

Description of Parameters

Parameter	Description	Value	Source
s_1	Recruitment rate of cats (birth and immigration.)	2.34	Assumed
τ	Natural death rate of cats.	0.43	Assumed
γ_1	Transmission rate from infected cats to susceptible cats.	0.23	Assumed
π	Vaccination rate of susceptible cats.	0.613	Assumed
ϑ_1	Waning rate of immunity in recovered cats.	0.3	Assumed
ϑ_2	Waning rate of vaccine induced immunity in vaccinated cats.	0.98	Assumed
γ_2	Progression rate from the first infection stage I_1 to the second I_2.	0.34	Assumed
β_1	Recovery rate from the first infection stage I_1.	0.123	Assumed
β_2	Recovery rate from the second infection stage I_2.	0.97	Assumed

Table 2: Description and values of model parameters

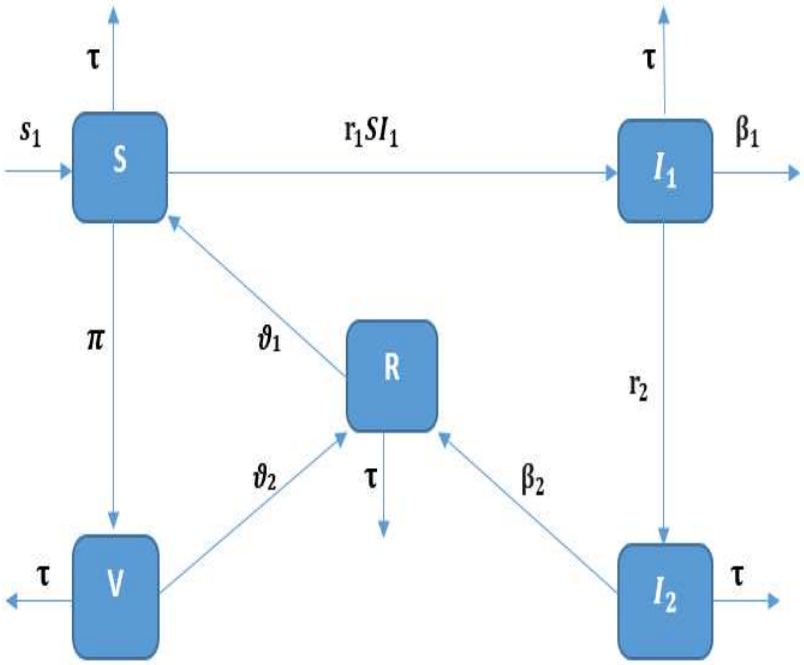

Fig. 1: The flow diagram shows proposed model.

The following is the construction of a mathematical framework with five dynamical variables, based on the structural depiction given in Figure 1 and considered variables including involved parameters given in table 1 and table 2 respectively. The following is the presentation of the suggested mathematical model under created assumption and objectives according to modeling basic principles including balance principle, We get:

$$\begin{cases} DS = s_1 + \vartheta_1 R - \gamma_1 SI_1 - \tau S - \pi S, \\ DV = \pi S - (\tau + \vartheta_2)V, \\ DI_1 = \gamma_1 SI_1 - (\tau + \gamma_2 + \beta_1)I_1, \\ DI_2 = \gamma_2 I_1 - (\tau + \beta_2)I_2, \\ DR = \vartheta_2 V + \beta_2 I_2 - (\tau + \vartheta_1)R. \end{cases} \tag{3}$$

The initial condition are;

$$S(0)=S^{\circ}\geq 0, V(0)=V^{\circ}\geq 0, I_1(0)=I^{\circ}\geq 0, I_2(0)=I^{\circ}\geq 0, R(0)=R^{\circ}\geq 0.$$

Where;
$S(0)>0, V(0)>0, I_1(0)>0, I_2>0, R(0)>0.$
Utilizing the definition of Atangana-Baleanu caputo operator above mathematical model is converted into fractional order model, given below;

$$\begin{cases} {}^{ABC}D_t^{\mu}S(t)=s_1+\vartheta_1 R-\gamma_1 SI_1-\tau S-\pi S,\\ {}^{ABC}D_t^{\mu}V(t)=\pi S-(\tau+\vartheta_2)V,\\ {}^{ABC}D_t^{\mu}I_1(t)=\gamma_1 SI_1-(\tau+\gamma_2+\beta_1)I_1,\\ {}^{ABC}D_t^{\mu}I_2(t)=\gamma_2 I_1-(\tau+\beta_2)I_2,\\ {}^{ABC}D_t^{\mu}R(t)=\vartheta_2 V+\beta_2 I_2-(\tau+\vartheta_1)R. \end{cases} \tag{4}$$

With initial Values;

$$S(0)=S^{\circ}\geq 0, V(0)=V^{\circ}\geq 0, I_1(0)=I^{\circ}\geq 0, I_2(0)=I^{\circ}\geq 0, R(0)=R^{\circ}\geq 0.$$

$$\begin{cases} {}^{ABC}D_t^{\mu}S(t)=d(t,Y(t)),\\ {}^{ABC}D_t^{\mu}V(t)=e(t,Y(t)),\\ {}^{ABC}D_t^{\mu}I_1(t)=f(t,Y(t)),\\ {}^{ABC}D_t^{\mu}I_2(t)=g(t,Y(t)),\\ {}^{ABC}D_t^{\mu}R(t)=h(t,Y(t)). \end{cases} \tag{5}$$

Assume that $Y(t)=(S,V,I_1,I_2,R)(t)$. Using the lemma and the starting conditions, we derive the following by applying the fractional operator ${}^{AB}I^{\mu}$ of the μ to both sides:

$$S(t)=S_0+\frac{1-\mu}{L(\mu)}d(t,Y(t))+\frac{\mu}{\Gamma(\mu)L(\mu)}\int_0^t(t-Z)^{\mu-1}d(Z,Y(z))dz,$$

$$V(t)=V_0+\frac{1-\mu}{L(\mu)}e(t,Y(t))+\frac{\mu}{\Gamma(\mu)L(\mu)}\int_0^t(t-Z)^{\mu-1}e(Z,Y(z))dz,$$

$$I_1(t)=I_0+\frac{1-\mu}{L(\mu)}f(t,Y(t))+\frac{\mu}{\Gamma(\mu)L(\mu)}\int_0^t(t-Z)^{\mu-1}f(Z,Y(z))dz,$$

$$I_2(t)=I_0+\frac{1-\mu}{L(\mu)}g(t,Y(t))+\frac{\mu}{\Gamma(\mu)L(\mu)}\int_0^t(t-Z)^{\mu-1}g(Z,Y(z))dz,$$

$$R(t)=R_0+\frac{1-\mu}{L(\mu)}h(t,Y(t))+\frac{\mu}{\Gamma(\mu)L(\mu)}\int_0^t(t-Z)^{\mu-1}h(Z,Y(z))dz.$$

Assume that $Y(t)=(S,V,I_1,I_2,R)(t)$ and $Y(z)=(S,V,I_1,I_2,R)(z)$. In order to prove the existence and uniqueness of solutions for the nonlinear mappings, several requirements have been put in place $d,e,f,g,h:[0,T]\times L\times L\longrightarrow L$.
Positive constants are present $K_d,K_e,K_f,K_g,K_h>0$ so that, for every $S,\overline{S},V,\overline{V},I_1,\overline{I_1},I_2,\overline{I_2},R,\overline{R}\in R$ the following circumstance is true:

$$|d(t,Y(t))-d(\bar{t},\overline{Y(t)})|\leq K_d[|S-\overline{S}|+|V-\overline{V}|+|I_1-\overline{I_1}|+|I_2-\overline{I_2}|+|R-\overline{R}|],$$

$$|e(t,Y(t))-e(\bar{t},\overline{Y(t)})|\leq K_e[|S-\overline{S}|+|V-\overline{V}|+|I_1-\overline{I_1}|+|I_2-\overline{I_2}|+|R-\overline{R}|],$$

$$|f(t,Y(t))-f(\bar{t},\overline{Y(t)})|\leq K_f[|S-\overline{S}|+|V-\overline{V}|+|I_1-\overline{I_1}|+|I_2-\overline{I_2}|+|R-\overline{R}|],$$

$$|g(t,Y(t))-g(\bar{t},\overline{Y(t)})|\leq K_g[|S-\overline{S}|+|V-\overline{V}|+|I_1-\overline{I_1}|+|I_2-\overline{I_2}|+|R-\overline{R}|],$$

$$|h(t,Y(t))-h(\bar{t},\overline{Y(t)})|\leq K_h[|S-\overline{S}|+|V-\overline{V}|+|I_1-\overline{I_1}|+|I_2-\overline{I_2}|+|R-\overline{R}|].$$

We consider the existence of constants $M_d, M_e, M_f, M_g, M_h, N_d, N_e, N_f, N_g, N_h, O_d, O_e, O_f, O_g, O_h, P_d, P_e, P_f, P_g, P_h > 0$ and $Q_d, Q_e, Q_f, Q_g, Q_h > 0$.

$$|d(t,Y(t))| \leq M_d|S| + N_d|S| + O_d|S| + P_d|S| + Q_d,$$
$$|d(t,Y(t))| \leq M_e|S| + N_e|S| + O_e|S| + P_e|S| + Q_e,$$
$$|d(t,Y(t))| \leq M_f|S| + N_f|S| + O_f|S| + P_f|S| + Q_f,$$
$$|d(t,Y(t))| \leq M_g|S| + N_g|S| + O_g|S| + P_g|S| + Q_g,$$
$$|d(t,Y(t))| \leq M_h|S| + N_h|S| + O_h|S| + P_h|S| + Q_h.$$

Theorem 3.1. Assuming the continuity of d, e, f, g, h along with the second assumption, the system admits at least one solution whenever $(\frac{1-\mu}{L(\mu)})\ K > 1$, where $K = \max\{K_d, K_e, K_f, K_g, K_h\}$.

Proof. Krasnoselskii's fixed point theorem can be used to prove that solutions exist. We present the operators $X = (X_1, X_2, X_3, X_4, X_5)$, $L = (L_1, L_2, L_3, L_4, L_5)$ which have the following definitions:

$$X_1Y(t) = S_0 + \frac{1-\mu}{L(\mu)} d(t,Y(t)),$$

$$L_1Y(t) = \frac{\mu}{\Gamma(\mu)L(\mu)} \int_0^t (t-Z)^{\mu-1} d(Z,Y(z))dz,$$

$$X_2V(t) = V_0 + \frac{1-\mu}{L(\mu)} e(t,Y(t)),$$

$$L_2V(t) = \frac{\mu}{\Gamma(\mu)L(\mu)} \int_0^t (t-Z)^{\mu-1} e(Z,Y(z))dz,$$

$$X_3I_1(t) = I_0 + \frac{1-\mu}{L(\mu)} f(t,Y(t)),$$

$$L_3I_1(t) = \frac{\mu}{\Gamma(\mu)L(\mu)} \int_0^t (t-Z)^{\mu-1} f(Z,Y(z))dz,$$

$$X_4I_2(t) = I_0 + \frac{1-\mu}{L(\mu)} g(t,Y(t)),$$

$$L_4I_2(t) = \frac{\mu}{\Gamma(\mu)L(\mu)} \int_0^t (t-Z)^{\mu-1} g(Z,Y(z))dz,$$

$$X_5R(t) = R_0 + \frac{1-\mu}{L(\mu)} h(t,Y(t)),$$

$$L_5R(t) = \frac{\mu}{\Gamma(\mu)L(\mu)} \int_0^t (t-Z)^{\mu-1} h(Z,Y(z))dz.$$

Where as $Y(t) = S(t), V(t), I_1(t), I_2(t), R(t)$ and $Y(z) = S(z), V(z), I_1(z), I_2(z), R(z)$ and $Y = (S, V, I_1, I_2, R)$. Consequently, it is demonstrated that X is a contraction operator and L is a continuous mapping. The following is true for any $Y = (\overline{S}, \overline{V}, \overline{I_1}, \overline{I_2}, \overline{R}) \in \gamma$, we have;

$$|X_1(t,Y(t)) - X_1(\bar{t}, \overline{Y(t)})| \leq K_d[|S-\overline{S}| + |V-\overline{V}| + |I_1-\overline{I_1}| + |I_2-\overline{I_2}| + |R-\overline{R}|],$$

Hence we obtain;

$$\|X_1(t,Y(t))-X_1(\bar{t},\overline{Y(t)})\| \leq K_d[\|S-\bar{S}\|+\|V-\bar{V}\|+\|I_1-\bar{I_1}\|+\|I_2(t)-\bar{I_2}\|+\|R-\bar{R}\|],$$

$$\|X_2(t,Y(t))-X_2(\bar{t},\overline{Y(t)})\| \leq K_e[\|S-\bar{S}\|+\|V-\bar{V}\|+\|I_1-\bar{I_1}\|+\|I_2-\bar{I_2}\|+\|R-\bar{R}\|],$$

$$\|X_3(t,Y(t))-X_3(\bar{t},\overline{Y(t)})\| \leq K_f[\|S-\bar{S}\|+\|V-\bar{V}\|+\|I_1-\bar{I_1}\|+\|I_2-\bar{I_2}\|+\|R-\bar{R}\|],$$

$$\|X_4(t,Y(t))-X_4(\bar{t},\overline{Y(t)})\| \leq K_g[\|S-\bar{S}\|+\|V-\bar{V}\|+\|I_1-\bar{I_1}\|+\|I_2-\bar{I_2}\|+\|R-\bar{R}\|],$$

$$\|X_5(t,Y(t))-X_5(\bar{t},\overline{Y(t)})\| \leq K_h[\|S-\bar{S}\|+\|V-\bar{V}\|+\|I_1-\bar{I_1}\|+\|I_2-\bar{I_2}\|+\|R-\bar{R}\|].$$

Thus;

$$\|X(t),Y(t)-\overline{X(t)},\overline{Y(t)}\| \leq \frac{1-\mu}{L(\mu)}[\|Y-(\bar{S},\bar{V},\bar{I_1},\bar{I_2},\bar{R})\|].$$

It can be seen from this that E is a contraction. The following definition and introduction of a closed subset C of Y are provided:

$$C = Y \in Y : \|Y\| \leq \beta, \beta > 0.$$

Assume that $Y = S,V,I_1,I_2,R$. Examine any $Y \in C$ to demonstrate that K is both continuous and compact. Then we get:

$$\|L_1(Y)\| \max_{t\in[0,T]} \frac{\mu}{\Gamma(\mu)L(\mu)} \int_0^t (t-Z)^{\mu-1} d(Z,Y(z))dz$$

$$\leq \frac{T^\mu}{\Gamma(\mu)L(\mu)}[M_d\|F\|+N_d\|F\|+O_d\|F\|+P_d\|F\|+Q_d],$$

$$\|L_2(Y)\| \max_{t\in[0,T]} \frac{\mu}{\Gamma(\mu)L(\mu)} \int_0^t (t-Z)^{\mu-1} d(Z,Y(z))dz$$

$$\leq \frac{T^\mu}{\Gamma(\mu)L(\mu)}[M_e\|G\|+N_e\|G\|+O_e\|G\|+P_e\|G\|+Q_e],$$

$$\|L_3(Y)\| \max_{t\in[0,T]} \frac{\mu}{\Gamma(\mu)L(\mu)} \int_0^t (t-Z)^{\mu-1} d(Z,Y(z))dz$$

$$\leq \frac{T^\mu}{\Gamma(\mu)L(\mu)}[M_f\|H\|+N_f\|H\|+O_f\|H\|+P_f\|H\|+Q_f],$$

$$\|L_4(Y)\| \max_{t\in[0,T]} \frac{\mu}{\Gamma(\mu)L(\mu)} \int_0^t (t-Z)^{\mu-1} d(Z,Y(z))dz$$

$$\leq \frac{T^\mu}{\Gamma(\mu)L(\mu)}[M_g\|I\|+N_g\|I\|+O_g\|I\|+P_g\|I\|+Q_g],$$

$$\|L_5(Y)\| \max_{t\in[0,T]} \frac{\mu}{\Gamma(\mu)L(\mu)} \int_0^t (t-Z)^{\mu-1} d(Z,Y(z))dz$$

$$\leq \frac{T^\mu}{\Gamma(\mu)L(\mu)}[M_h\|J\|+N_h\|J\|+O_h\|J\|+P_h\|J\|+Q_h],$$

Thus;

$$\|L(Y)\| \leq T^\mu \frac{[(M_1+N_1+O_1+P_1)\beta+Q_1]}{L(\mu)\Gamma(\mu)} = \mu.$$

Where $M_1 = M_d+M_e+M_f+M_g+M_h, N_1 = N_d+N_e+N_f+N_g+N_h, O_1 = O_d+O_e+O_f+O_g+O_h$. Then we show that X is continuous after establishing that X is bounded. Let $t_1 < t_2 \in [0,1]$ then consider:

$$|L_1(Y)(t_2)-L_1(Y)(t_1)| = \frac{\mu}{\Gamma(\mu)L(\mu)} \times |\int_0^{t_2} (t_2-z)^{\mu-1} d(Y(z))dz - \int_0^{t_1} (t_1-z)^{\mu-1} d(Y(z))dz|$$

$$\leq \frac{\mu}{\Gamma(\mu)L(\mu)}[\int_0^{t_2}(t_2-z)^{\mu-1}-\int_0^{t_1}(t_1-z)^{\mu-1}]((M_d+N_d+O_d+P_d)\beta+Q_d)ds,$$

$$\leq \frac{((M_1+N_1+O_1+P_1)\beta+Q_1)}{L(\mu)\Gamma(\mu)}[t_2^{\mu}-t_1^{\mu}],$$

$$|L_1(Y)(t_2)-L_1(Y)(t_1)| \leq \frac{((M_d+N_d+O_d+P_d)\beta+Q_d)}{L(\mu)\Gamma(\mu)}[t_2^{\mu}-t_1^{\mu}],$$

$$|L_2(Y)(t_2)-L_2(Y)(t_1)| \leq \frac{((M_e+N_e+O_e+P_e)\beta+Q_e)}{L(\mu)\Gamma(\mu)}[t_2^{\mu}-t_1^{\mu}],$$

$$|L_3(Y)(t_2)-L_3(Y)(t_1)| \leq \frac{((M_f+N_f+O_f+P_f)\beta+Q_f)}{L(\mu)\Gamma(\mu)}[t_2^{\mu}-t_1^{\mu}],$$

$$|L_4(Y)(t_2)-L_4(Y)(t_1)| \leq \frac{((M_g+N_g+O_g+P_g)\beta+Q_g)}{L(\mu)\Gamma(\mu)}[t_2^{\mu}-t_1^{\mu}],$$

$$|L_5(Y)(t_2)-L_5(Y)(t_1)| \leq \frac{((M_h+N_h+O_h+P_h)\beta+Q_h)}{L(\mu)\Gamma(\mu)}[t_2^{\mu}-t_1^{\mu}].$$

$\|L_1(Y)(t_2)-L_1(Y)(t_1)\| \to 0$ as $t_1 \to t_2$, $\|L_2(Y)(t_2)-L_2(Y)(t_1)\| \to 0$ as $t_1 \to t_2$, $\|L_3(Y)(t_2)-L_3(Y)(t_1)\| \to 0$ as $t_1 \to t_2$, $\|L_4(Y)(t_2)-L_4(Y)(t_1)\| \to 0$ as $t_1 \to t_2$, $\|L_5(Y)(t_2)-L_5(Y)(t_1)\| \to 0$ as $t_1 \to t_2$.
Consequently, it is proven that G functions as an continuous operator. Through the use of the Arzelà-Ascoli theorem, it has already been shown that L is uniformly bounded and completely continuous. As a result, K admits a unique solution and is comparatively compact.

Theorem 3.2. The T. gondii Transmission with Vaccination and Sanitation system involving the ABC derivative has a unique solution under the first assumption.

$$\frac{5T^{\mu}}{L(\mu)\Gamma(\mu)}K < 1.$$

With $\max\{K_d, K_e, K_f, K_g, K_h\} = K$.

Proof. Define the operator $\dot{Z} = (Z_1, Z_2, Z_3, Z_4, Z_5) : Y \to Y$ as;

$$Z_1Y(t) = F_0 + \frac{1-\mu}{L(\mu)}d(t,Y(t)) + \frac{\mu}{\Gamma(\mu)L(\mu)}\int_0^t (t-z)^{\mu-1}d(z,Y(z))dz,$$

$$Z_2Y(t) = G_0 + \frac{1-\mu}{L(\mu)}e(t,Y(t)) + \frac{\mu}{\Gamma(\mu)L(\mu)}\int_0^t (t-z)^{\mu-1}e(z,Y(z))dz,$$

$$Z_3Y(t) = H_0 + \frac{1-\mu}{L(\mu)}f(t,Y(t)) + \frac{\mu}{\Gamma(\mu)L(\mu)}\int_0^t (t-z)^{\mu-1}f(z,Y(z))dz,$$

$$Z_4Y(t) = I_0 + \frac{1-\mu}{L(\mu)}g(t,Y(t)) + \frac{\mu}{\Gamma(\mu)L(\mu)}\int_0^t (t-z)^{\mu-1}g(z,Y(z))dz,$$

$$Z_5Y(t) = J_0 + \frac{1-\mu}{L(\mu)}h(t,Y(t)) + \frac{\mu}{\Gamma(\mu)L(\mu)}\int_0^t (t-z)^{\mu-1}h(z,Y(z))dz,$$

Where $Y = (S,V,I_1,I_2,R)$, $Y(t) = (S,V,I_1,I_2,R)(t)$ and $Y(z) = (S,V,I_1,I_2,R)(z)$. Now we take $Y = (S,V,I_1,I_2,R)$ and $\overline{Y} = (\overline{S},\overline{V},\overline{I_1},\overline{I_2},\overline{R})$ we have;

$$\|Z_1(Y)-Z_1(\overline{Y})\| = \max_{t\in[0,T]}|\frac{\mu}{\Gamma(\mu)L(\mu)}\int_0^t (t-z)^{\mu-1}[d(z,Y(z))-d(\overline{z},\overline{Y(z)})]|,$$

$$\leq \frac{T_{\mu}}{L(\mu)\Gamma(\mu)}K_d[\|S-\overline{S}\|+\|V-\overline{V}\|+\|I_1-\overline{I_1}\|+\|I_2-\overline{I_2}\|+\|R-\overline{R}\|],$$

$$\|Z_2(Y)-Z_2(\overline{Y})\| \leq \frac{T_{\mu}}{L(\mu)\Gamma(\mu)}K_e[\|S-\overline{S}\|+\|V-\overline{V}\|+\|I_1-\overline{I_1}\|+\|I_2-\overline{I_2}\|+\|R-\overline{R}\|],$$

$$\|Z_3(Y)-Z_3(\overline{Y})\| \leq \frac{T_{\mu}}{L(\mu)\Gamma(\mu)}K_f[\|S-\overline{S}\|+\|V-\overline{V}\|+\|I_1-\overline{I_1}\|+\|I_2-\overline{I_2}\|+\|R-\overline{R}\|],$$

$$\|Z_4(Y)-Z_4(\overline{Y})\| \leq \frac{T_\mu}{L(\mu)\Gamma(\mu)}K_g[\|S-\overline{S}\|+\|V-\overline{V}\|+\|I_1-\overline{I_1}\|+\|I_2-\overline{I_2}\|+\|R-\overline{R}\|],$$

$$\|Z_5(Y)-Z_5(\overline{Y})\| \leq \frac{T_\mu}{L(\mu)\Gamma(\mu)}K_h[\|S-\overline{S}\|+\|V-\overline{V}\|+\|I_1-\overline{I_1}\|+\|I_2-\overline{I_2}\|+\|R-\overline{R}\|],$$

$$\|Z(Y)-(\overline{Z(Y)})\| = \frac{5T^\mu}{L(\mu)\Gamma(\mu)}K\|Y-\overline{Y}\|.$$

Consequently, the contraction property is satisfied by Z. The system guarantees uniqueness by admitting a single, well-defined solution according to the Banach fixed-point theorem. We then go on to formulate the Ulam-Hyers stability criterion after proving this conclusion.

Theorem 3.3. The solution of the proposed model exhibits Ulam-Hyers stability provided that the spectral radius of the associated matrix satisfies the Ulam-Hyers stability condition.

$$\begin{pmatrix} f & f & f \\ g & g & g \\ h & h & h \\ i & i & i \\ j & j & j \end{pmatrix}$$

The result of $|f+g+h+i+j|=1$ where;

$$f = \frac{(1-\mu)}{L(\mu)} + \frac{T^\mu}{(L(\mu)\Gamma(\mu))}K_d,$$

$$g = \frac{(1-\mu)}{L(\mu)} + \frac{T^\mu}{(L(\mu)\Gamma(\mu))}K_e,$$

$$h = \frac{(1-\mu)}{L(\mu)} + \frac{T^\mu}{(L(\mu)\Gamma(\mu))}K_f,$$

$$i = \frac{(1-\mu)}{L(\mu)} + \frac{T^\mu}{(L(\mu)\Gamma(\mu))}K_g,$$

$$j = \frac{(1-\mu)}{L(\mu)} + \frac{T^\mu}{(L(\mu)\Gamma(\mu))}K_h.$$

Proof. Assume that Y is an arbitrary model solution, and $\overline{Y}$ the system's corresponding unique solution, which is written as

$$\|Y-\overline{Y}\| \leq \begin{pmatrix} f & f & f \\ g & g & g \\ h & h & h \\ i & i & i \\ j & j & j \end{pmatrix} \begin{pmatrix} \|S-\overline{S}\| \\ \|V-\overline{V}\| \\ \|I_1-\overline{I_1}\| \\ \|I_2-\overline{I_2}\| \\ \|R-\overline{R}\| \end{pmatrix} \tag{6}$$

Therefore, the model maintains stability.

3 Mathematical Model With Fractional Operator ABC

Study the model written in ABC operator format as:

$$\begin{cases} {}^{ABC}D_t^\mu(S(t))_S = s_1+\vartheta_1 R-\gamma_1 SI_1-\tau S-\pi S, \\ {}^{ABC}D_t^\mu(V(t))_V = \pi S-(\tau+\vartheta_2)V, \\ {}^{ABC}D_t^\mu(I_1(t))_I = \gamma_1 SI_1-(\tau+\gamma_2+\beta_1)I_1, \\ {}^{ABC}D_t^\mu(I_2(t))_I = \gamma_2 I_1-(\tau+\beta_2)I_2, \\ {}^{ABC}D_t^\mu(R(t))_R = \vartheta_2 V+\beta_2 I_2-(\tau+\vartheta_1)R. \end{cases} \tag{7}$$

Where;

$$S(0) \geq 0, V(0) \geq 0, I_1(0) \geq 0, I_2(0) \geq 0, R(0) \geq 0.$$

Theorem 3.4. In R_+^5, Under the specified beginning conditions, the solution of the fractal-fractional model under consideration is bounded and unique.

Proof.

$$\begin{cases} {}^{ABC}D_t^{\mu}(S(t))_{S=0} > 0, \\ {}^{ABC}D_t^{\mu}(V(t))_{V=0} > 0, \\ {}^{ABC}D_t^{\mu}(I_1(t))_{I=0} > 0, \\ {}^{ABC}D_t^{\mu}(I_2(t))_{I=0} > 0, \\ {}^{ABC}D_t^{\mu}(R(t))_{R=0} > 0. \end{cases} \tag{8}$$

If the first requirement is met $(S(0), V(0), I_1(0), I_2(0), R(0)) \in R_+^5$. Consequently, the trajectory stays contained within this non-negative area. Additionally, the related vector field is oriented inward along the nonnegative orthant's border, suggesting that R_+^5, is a set that is positively invariant.

3.1 Existence and Uniqueness

Fixed-point theory was used to prove that at least one unique solution existed. Consequently,

$$\begin{cases} {}_0^{ABR}D_{0,t}^{\mu,\upsilon}(S(t)) = \upsilon t^{\upsilon-1}F(K_1), \\ {}_0^{ABR}D_{0,t}^{\mu,\upsilon}(V(t)) = \upsilon t^{\upsilon-1}G(K_1), \\ {}_0^{ABR}D_{0,t}^{\mu,\upsilon}(I_1(t)) = \upsilon t^{\upsilon-1}H(K_1), \\ {}_0^{ABR}D_{0,t}^{\mu,\upsilon}(I_2(t)) = \upsilon t^{\upsilon-1}I(K_1), \\ {}_0^{ABR}D_{0,t}^{\mu,\upsilon}(R(t)) = \upsilon t^{\upsilon-1}J(K_1). \end{cases} \tag{9}$$

As $K_1 = (t, S, V, I_1, I_2, R)$ Where;

$$\begin{cases} F(K_1) = s_1 + \vartheta_1 R - \gamma_1 S I_1 - \tau S - \pi S, \\ G(K_1) = \pi S - (\tau + \vartheta_2)V, \\ H(K_1) = \gamma_1 S I_1 - (\tau + \gamma_2 + \beta_1)I_1, \\ I(K_1) = \gamma_2 I_1 - (\tau + \beta_2)I_2, \\ J(K_1) = \vartheta_2 V + \beta_2 I_2 - (\tau + \vartheta_1)R. \end{cases} \tag{10}$$

We can write system as;

$$\begin{cases} {}_0^{ABR}D_t^{\mu} = \mu t^{\mu-1}\mu(t, \varepsilon(t)), \\ \varepsilon(0) = \varepsilon_0. \end{cases} \tag{11}$$

By replacing ${}_0^{ABR}D_t^{\mu,\upsilon}$ by ${}^{ABC}D_t^{\alpha}$ and applying FI, we obtain;

$$\varepsilon(t) = \varepsilon(0) + \frac{\varphi t^{\varphi-1}(1-\mu)}{CB(\mu)}\Lambda(t, \varepsilon(t)) + \frac{\mu\varphi}{CB(\mu)\Gamma(\mu)}$$

Making a substitution for ${}_0^{ABR}D_t^{\mu,\upsilon}$ by ${}^{ABC}D_t^{\alpha}$ and we arrive to the following using the fractional integral operator:

$$\varepsilon(t) = \varepsilon(0) + \frac{\upsilon t^{\upsilon-1}(1-\mu)}{MN(\mu)}\Upsilon(t, \varepsilon(t)) + \frac{\mu\upsilon}{MN(\mu)\Gamma(\mu)}\int_0^t \mu^{\upsilon-1}(t-\mu)\Upsilon(t, \varepsilon(t))d\mu,$$

$$\varepsilon(t)=\begin{cases} S(t)\\ V(t)\\ I_1(t)\\ I_2(t)\\ R(t)\end{cases},\varepsilon(0)=\begin{cases} S(0)\\ V(0)\\ I_1(0)\\ I_2(0)\\ R(0)\end{cases},\Upsilon(t,\varepsilon(t))=\begin{cases} F(K_1),\\ G(K_1),\\ H(K_1),\\ I(K_1),\\ J(K_1).\end{cases}$$

As is often believed, the Banach space $C=K\times K$ is taken into consideration in the context of existence theory, where the interval is provided by $K=[0,T]$.

$$\|\varepsilon\|=\max_{t\in[0,T]}|S(t)+V(t)+I_1(t)+I_2(t)+R(t)|.$$

Define $\kappa:C\to C$

$$\kappa(\varepsilon)(t)=\varepsilon(0)+\frac{\upsilon t^{\upsilon-1}(1-\mu)}{MN(\mu)}\Upsilon(t,\varepsilon(t))+\frac{\mu\upsilon}{MN(\mu)\Gamma(\mu)}\int_0^t\mu^{\upsilon-1}(t-\mu)\Upsilon(t,\varepsilon(t))d\mu.$$

Assume that the nonlinear function $\Upsilon(t,\varepsilon(t))$ satisfies the requirements.
• For all $\varepsilon\in C$, $\exists$ constant F_Υ and R_Υ such as;

$$|\Upsilon(t,\varepsilon(t))|\leq F_\Upsilon|\varepsilon(t)+R_\Upsilon. \tag{12}$$

$$|\Upsilon(t,\varepsilon(t))-\Lambda(t,\overline{\varepsilon}(t))|\leq X_\Lambda|\varepsilon(t)-\overline{\varepsilon}(t)|. \tag{13}$$

Theorem 3.5. Assume that (14) holds true. Allow to be a continuous function and $\Upsilon=[0,T]\times C\to P$. At least one solution is then admitted by the model.
Proof. As stated in equation (13), we first show that the operator κ is completely continuous. Given that Υ is continuous, κ must also be continuous. Let $K=\varepsilon\in C:\|\varepsilon\|\leq P,P>0$. Now for any $\varepsilon\in C$, We have;

$$|\kappa(\varepsilon)|=\max_{t\in[0,T]}|\varepsilon(0)+\frac{\upsilon t^{\upsilon-1}(1-\mu)}{MN(\mu)}\Upsilon(t,\varepsilon(t))+\frac{\mu\upsilon}{MN(\mu)\Gamma(\mu)}\int_0^t\mu^{\upsilon-1}(t-\mu)\Upsilon(t,\varepsilon(t))d\mu.$$

$$\leq\varepsilon(0)+\frac{\upsilon Bt^{\upsilon-1}(1-\mu)}{MN(\mu)}(F_\Upsilon\|\varepsilon\|+R_\Upsilon)+\max_{t\in[0,T]}\frac{\mu\upsilon}{MN(\mu)\Gamma(\mu)}\int_0^t\mu^{\upsilon-1}(t-\mu)\mid\Upsilon(t,\varepsilon(t))\mid d\mu.$$

$$\leq\varepsilon(0)+\frac{\upsilon Bt^{\upsilon-1}(1-\mu)}{MN(\mu)}(F_\Upsilon\|\varepsilon\|+R_\Upsilon)+\frac{\mu\upsilon}{MN(\mu)\Gamma(\mu)}(F_\Upsilon\|\varepsilon\|+R_\Upsilon)B^{\mu+\upsilon-1}K(\mu,\upsilon)\leq P. \tag{14}$$

Despite the regular boundedness of κ the function $K(\mu,\upsilon)$ is likewise continuous. Let $t_1<t_2\leq T$ to demonstrate the equicontinuity of $\Re$ is used as an example. Then we consider:

$$|\kappa(\varepsilon)(t_2)-\kappa(\varepsilon)(t_1)|=|\frac{\upsilon t_2^{\upsilon-1}(1-\mu)}{MN(\mu)}\Upsilon(t_2,\varepsilon(t_2))+\frac{\mu\upsilon}{MN(\mu)\Gamma(\mu)}\int_0^{t_2}\mu^{\upsilon-1}(t_2-\mu)\Upsilon(\mu,\varepsilon(\mu))d\mu$$

$$-\frac{\upsilon t_1^{\upsilon-1}(1-\mu)}{MN(\mu)}\Upsilon(t_1,\varepsilon(t_1))+\frac{\mu\upsilon}{MN(\mu)\Gamma(\mu)}\int_0^{t_2}\mu^{\upsilon-1}(t_2-\mu)\Upsilon(\mu,\varepsilon(\mu))d\mu\mid$$

$$\leq|\frac{\upsilon t_2^{\upsilon-1}(1-\mu)}{MN(\mu)}(F_\Upsilon\mid\varepsilon(t)\mid,R_F)+\frac{\mu\upsilon}{MN(\mu)\Gamma(\mu)}(F_\Upsilon\mid\varepsilon(t)\mid,R_F)t_2^{\mu+\upsilon-1}L(\mu,\varepsilon)\mid$$

$$-\frac{\upsilon t_1^{\upsilon-1}(1-\mu)}{MN(\mu)}(F_\Upsilon\mid\varepsilon(t)\mid,R_F)+\frac{\mu\upsilon}{MN(\mu)\Gamma(\mu)}(F_\Upsilon\mid\varepsilon(t)\mid,R_F)t_1^{\mu+\upsilon-1}L(\mu,\varepsilon)\mid \tag{15}$$

When $t_1\to t_2$ then $|\kappa(\varepsilon)(t_2)-\kappa(\varepsilon)(t_1)|$. Hence we conclude that;

$$\|\kappa(\varepsilon)t_2-\kappa(\varepsilon)t_1\|\to0,t_1\to t_2. \tag{16}$$

Thus κ is continuous, bringing the evidence to a close.
Theorem 3.6. Suppose that if $\alpha < 1$ here;

$$\alpha = (\frac{\upsilon B^{\upsilon-1}(1-\mu)}{MN(\mu)} + \frac{\mu\upsilon}{MN(\mu)\Gamma(\mu)} B^{\mu+\upsilon-1} K(\mu,\upsilon))J_{\Upsilon}. \tag{17}$$

The model under consideration admits a unique solution.
Proof. Take $\varepsilon, \overline{\varepsilon} \in C$ we get;

$$|\kappa(\varepsilon)-\kappa(\overline{\varepsilon})| = \max_{t\in[0,T]} |\frac{\upsilon t^{\upsilon-1}(1-\mu)}{MN(\mu)}(\Upsilon(t,\varepsilon(t))-\Upsilon(t,\overline{\varepsilon(t)})) + \frac{\mu\upsilon}{MN(\mu)\Gamma(\mu)}\int_0^t \mu^{\upsilon-1}(t-\mu)^{\upsilon-1} d\mu(\Upsilon(\mu,\varepsilon(\mu))-\Upsilon(\mu,\overline{\varepsilon(\mu)}))|,$$

$$\leq [\frac{\upsilon B^{\upsilon-1}(1-\mu)}{MN(\mu)} + \frac{\mu\upsilon}{MN(\mu)\Gamma(\mu)} B^{\mu+\upsilon-1} K(\mu,\upsilon)]\|\varepsilon-\overline{\varepsilon}\|,$$

$$\leq \alpha\|\varepsilon-\varepsilon\|. \tag{18}$$

As a result, the contraction property is satisfied by α is a unique solution is admitted by the suggested model according to the Banach Contraction Principle.

3.2 Existence and Stability Theory

Using the fractal fractional operator in the ABC sense, we investigate the model's existence and uniqueness in this section. Assume:

$$\begin{aligned}
{}^{ABC}D_t^{\mu}(S(t)) &= s_1 + \vartheta_1 R - \gamma_1 S I_1 - \tau S - \pi S,\\
{}^{ABC}D_t^{\mu}(V(t)) &= \pi S - (\tau+\vartheta_2)V,\\
{}^{ABC}D_t^{\mu}(I_1(t)) &= \gamma_1 S I_1 - (\tau+\gamma_2+\beta_1)I_1,\\
{}^{ABC}D_t^{\mu}(I_2(t)) &= \gamma_2 I_1 - (\tau+\beta_2)I_2,\\
{}^{ABC}D_t^{\mu}(R(t)) &= \vartheta_2 V + \beta_2 I_2 - (\tau+\vartheta_1)R.
\end{aligned}$$

3.3 Positivity and Boundedness

This part offers a thorough analysis of the key elements to guarantee that the outcomes are understandable and unambiguous. In order to assess and validate the model's structure's validity and importance, the part looks at several methods.
Define the norm;

$$\| \phi \|_{\infty} = \sup_{t\varepsilon D_{\phi}} | \phi(t) | \tag{19}$$

Assume that D_{ϕ} denotes $\grave{\phi}$ domain. Therefore, the classical derivative's outcome is:

$$S(t) = s_1 + \vartheta_1 R - \gamma_1 S I_1 - \tau S - \pi S, \forall t \geq 0,$$

$$S(t) \geq -(\gamma_1 I_1 + \tau + \pi)S, \forall t \geq 0,$$

$$S(t) \geq -(\gamma_1 \sup_{t\varepsilon D_S} | I_1 | + \tau + \pi)S, \forall t \geq 0,$$

$$S(t) \geq -(\gamma_1 \| I_1 \| + \tau + \pi)S, \forall t \geq 0,$$

$$S(t) \geq S_o e^{-(\gamma_1 \|I_1\| + \tau + \pi)t}, \forall t \geq 0.$$

The following inequality is satisfied by the function $V(t)$:

$$V(t) = \pi S - (\tau + \vartheta_2)V, \forall t \geq 0,$$

$$V(t) \geq -(\tau + \vartheta_2)V, \forall t \geq 0,$$

$$V(t) \geq V_o(t) e^{-(\tau+\vartheta_2)t}, \forall t \geq 0.$$

The function $I_1(t)$ satisfies the following inequality:

$$I_1(t) = \gamma_1 S I_1 - (\tau + \gamma_2 + \beta_1)I_1, \forall t \geq 0,$$

$$I_1(t) \geq -(\tau + \gamma_2 + \beta_1)I_1, \forall t \geq 0,$$

$$I_1(t) \geq I_o e^{-(\tau+\gamma_2+\beta_1)t}, \forall t \geq 0.$$

The function $I_2(t)$ satisfies the following inequality:

$$I_2(t) = \gamma_2 I_1 - (\tau + \beta_2)I_2, \forall t \geq 0,$$

$$I_2(t) \geq -(\tau + \beta_2)I_2, \forall t \geq 0,$$

$$I_2(t) \geq I_o e^{-(\tau+\beta_2)t}, \forall t \geq 0.$$

The following inequality is satisfied by the function R(t):

$$R(t) = \vartheta_2 V + \beta_2 I_2 - (\tau + \vartheta_1)R, \forall t \geq 0,$$

$$R(t) \geq -(\tau + \vartheta_1)R, \forall t \geq 0,$$

$$R(t) \geq R_o e^{-(\tau+\vartheta_1)t}, \forall t \geq 0.$$

4 Analysis of Equilibrium points and Flip Bifurcation analysis

In this section, we will look into stable places. Through the identification of its constant states, formulation (3) becomes zero.

$$\begin{aligned}
{}^{ABC}D_t^{\mu} S(t) &= s_1 + \vartheta_1 R - \gamma_1 S I_1 - \tau S - \pi S, \\
{}^{ABC}D_t^{\mu} V(t) &= \pi S - (\tau + \vartheta_2)V, \\
{}^{ABC}D_t^{\mu} I_1(t) &= \gamma_1 S I_1 - (\tau + \gamma_2 + \beta_1)I_1, \\
{}^{ABC}D_t^{\mu} I_2(t) &= \gamma_2 I_1 - (\tau + \beta_2)I_2, \\
{}^{ABC}D_t^{\mu} R(t) &= \vartheta_2 V + \beta_2 I_2 - (\tau + \vartheta_1)R.
\end{aligned}$$

The disease-free equilibrium points of mathematical model:

$$T_1(S,V,I_1,I_2,R) = \begin{cases} S \to \frac{s_1(\tau+\eta_1)(\tau+\eta_2)}{\tau w}, \\ V \to \frac{\pi s_1(\tau+\eta_1)}{\tau w}, \\ I_1 \to 0, \\ I_2 \to 0, \\ R \to \frac{\pi s_1 \eta_2}{\tau w}. \end{cases} \tag{20}$$

Where;

$$w = \tau^2 + \tau t + \tau\eta_1 + \pi\eta_1 + \tau\eta_2 + \pi\eta_2 + \eta_1\eta_2 \tag{21}$$

After substituting the parameters values we get;

$$S \to 5.33538, V \to 0.0443478, I_1 \to 0, I_2 \to 0, R \to 0.0785787. \tag{22}$$

4.1 Local Stability

Eigenvalue calculations are used to evaluate the system's local stability. The suggested model demonstrates asymptotic stability when each eigenvalue is negative.

Theorem3.7. If $\arg(\lambda j < 1)$, the suggested fractional order model (3) exhibits local asymptotic stability.

Proof. Consider the Jacobian matrix for the developed fractional order model as given below:

$$J = \begin{pmatrix} \frac{\partial f_1}{\partial S} & \frac{\partial f_1}{\partial V} & \frac{\partial f_1}{\partial I_1} & \frac{\partial f_1}{\partial I_2} & \frac{\partial f_1}{\partial R} \\ \frac{\partial f_2}{\partial S} & \frac{\partial f_2}{\partial V} & \frac{\partial f_2}{\partial I_1} & \frac{\partial f_2}{\partial I_2} & \frac{\partial f_2}{\partial R} \\ \frac{\partial f_3}{\partial S} & \frac{\partial f_3}{\partial V} & \frac{\partial f_3}{\partial I_1} & \frac{\partial f_3}{\partial I_2} & \frac{\partial f_3}{\partial R} \\ \frac{\partial f_4}{\partial S} & \frac{\partial f_4}{\partial V} & \frac{\partial f_4}{\partial I_1} & \frac{\partial f_4}{\partial I_2} & \frac{\partial f_4}{\partial R} \\ \frac{\partial f_5}{\partial S} & \frac{\partial f_5}{\partial V} & \frac{\partial f_5}{\partial I_1} & \frac{\partial f_5}{\partial I_2} & \frac{\partial f_5}{\partial R} \end{pmatrix}$$

$$J = \begin{pmatrix} -\gamma_1 I_1 - (\tau+\pi) & 0 & -\gamma_1 S & 0 & \vartheta_1 \\ \pi & -(\tau+\vartheta_2) & 0 & 0 & 0 \\ \gamma_1 I_1 & 0 & \gamma_1 S - (\tau+\gamma_2+\beta_1) & 0 & 0 \\ 0 & 0 & \gamma_2 & -(\tau+\beta_2) & 0 \\ 0 & \vartheta_2 & 0 & \beta_2 & -(\tau+\vartheta_1) \end{pmatrix}$$

When the disease-free equilibrium point is applied, the Jacobian matrix takes the form:

$$J(E^*) = \begin{pmatrix} -(\tau+\pi) & 0 & \frac{-\gamma_1 s_1(\tau+\eta_1)(\tau+\eta_2)}{\tau(\tau^2+\tau t+\tau\eta_1+\pi\eta_1+\tau\eta_2+\pi\eta_2+\eta_1\eta_2)} & 0 & \vartheta_1 \\ \pi & -(\tau+\vartheta_2) & 0 & 0 & 0 \\ 0 & 0 & \frac{\gamma_1 s_1(\tau+\eta_1)(\tau+\eta_2)}{\tau(\tau^2+\tau t+\tau\eta_1+\pi\eta_1+\tau\eta_2+\pi\eta_2+\eta_1\eta_2)} - (\tau+\gamma_2+\beta_1) & 0 & 0 \\ 0 & 0 & \gamma_2 & -(\tau+\beta_2) & 0 \\ 0 & \vartheta_2 & 0 & \beta_2 & -(\tau+\vartheta_1) \end{pmatrix}$$

Now, Using the characteristics equation* as given below:

$$| J(E^*) - \lambda I | = 0$$

Using the above characteristics equation* we get as follows:

$$\begin{vmatrix} -(\tau+\pi)-\lambda & 0 & -\frac{\gamma_1 s_1(\tau+\eta_1)(\tau+\eta_2)}{\tau(\tau^2+\tau t+\tau\eta_1+\pi\eta_1+\tau\eta_2+\pi\eta_2+\eta_1\eta_2)} & 0 & \vartheta_1 \\ \pi & -(\tau+\vartheta_2)-\lambda & 0 & 0 & 0 \\ 0 & 0 & \frac{\gamma_1 s_1(\tau+\eta_1)(\tau+\eta_2)}{\tau(\tau^2+\tau t+\tau\eta_1+\pi\eta_1+\tau\eta_2+\pi\eta_2+\eta_1\eta_2)} - (\tau+\gamma_2+\beta_1)-\lambda & 0 & 0 \\ 0 & 0 & \gamma_2 & -(\tau+\beta_2)-\lambda & 0 \\ 0 & \vartheta_2 & 0 & \beta_2 & -(\tau+\vartheta_1)-\lambda \end{vmatrix} = 0 \tag{23}$$

Now solving the above determinant for λ, we get eigenvalues , which are given as:

$$\begin{cases} \lambda_1 = -(\tau+\pi), \\ \lambda_2 = -(\tau+\vartheta_2), \\ \lambda_3 = -(\tau+\gamma_2+\beta_1) + \frac{\gamma_1 s_1(\tau+\eta_1)(\tau+\eta_2)}{\tau(\tau^2+\tau t+\tau\eta_1+\pi\eta_1+\tau\eta_2+\pi\eta_2+\eta_1\eta_2)}, \\ \lambda_4 = -(\tau+\beta_2), \\ \lambda_5 = -(\tau+\vartheta_1). \end{cases} \tag{24}$$

Because each eigenvalue has a negative real part, the newly developed model is locally stable.

4.2 Flip bifurcation analysis

Our developed framework makes it clear that if: $(\vartheta,\gamma_1,\tau,\pi,\vartheta_2,\gamma_2,\beta_1,\beta_2)$ indicates the fixed set of variables, then no characteristic values are present. 1 and -1 may indicate that the division may disappear belongs to the designated collection:

$$(\vartheta,\gamma_1,\tau,\pi,\vartheta_2,\gamma_2,\beta_1,\beta_2)\in F|E(\frac{s_1(\tau+\eta_1)(\tau+\eta_2)}{\tau(\tau^2+\tau t+\tau\eta_1+\pi\eta_1+\tau\eta_2+\pi\eta_2+\eta_1\eta_2)},$$

$$\frac{\pi s_1(\tau+\eta_1)}{\tau(\tau^2+\tau t+\tau\eta_1+\pi\eta_1+\tau\eta_2+\pi\eta_2+\eta_1\eta_2)},\frac{\pi s_1\eta_2}{\tau(\tau^2+\tau t+\tau\eta_1+\pi\eta_1+\tau\eta_2+\pi\eta_2+\eta_1\eta_2)})$$

Theorem 3.8. The branching in our framework (3) does not end at:

$$T_1(S,V,I_1,I_2,R)=\begin{cases}S\to\frac{s_1(\tau+\eta_1)(\tau+\eta_2)}{\tau(\tau^2+\tau t+\tau\eta_1+\pi\eta_1+\tau\eta_2+\pi\eta_2+\eta_1\eta_2)},\\ V\to\frac{\pi s_1(\tau+\eta_1)}{\tau(\tau^2+\tau t+\tau\eta_1+\pi\eta_1+\tau\eta_2+\pi\eta_2+\eta_1\eta_2)},\\ I_1\to 0,\\ I_2\to 0,\\ R\to\frac{\pi s_1\eta_2}{\tau(\tau^2+\tau t+\tau\eta_1+\pi\eta_1+\tau\eta_2+\pi\eta_2+\eta_1\eta_2)}.\end{cases}$$

If a fixed set of variables is supplied:

$$(\vartheta,\gamma_1,\tau,\pi,\vartheta_2,\gamma_2,\beta_1,\beta_2)\in F|E(\frac{s_1(\tau+\eta_1)(\tau+\eta_2)}{\tau(\tau^2+\tau t+\tau\eta_1+\pi\eta_1+\tau\eta_2+\pi\eta_2+\eta_1\eta_2)},$$

$$\frac{\pi s_1(\tau+\eta_1)}{\tau(\tau^2+\tau t+\tau\eta_1+\pi\eta_1+\tau\eta_2+\pi\eta_2+\eta_1\eta_2)},\frac{\pi s_1\eta_2}{\tau(\tau^2+\tau t+\tau\eta_1+\pi\eta_1+\tau\eta_2+\pi\eta_2+\eta_1\eta_2)})$$

Proof. Since the equations in our model remain unchanged when I_1 and I_2 are set to 0, we aim to determine whether the proposed mathematical model exhibits a bifurcation at I_1 and $I_2=0$.

$$S_{t+1}=s_1+\vartheta_1 R-\tau S-\pi S \tag{25}$$

Indicates the map (15).

$$f(S)=s_1+\vartheta_1 R-\tau S-\pi S$$

$$\frac{\partial f}{\partial S}=-(\tau+\pi)$$

$$\frac{\partial f}{\partial \tau}=-S=-\frac{s_1(\tau+\eta_1)(\tau+\eta_2)}{\tau(\tau^2+\tau t+\tau\eta_1+\pi\eta_1+\tau\eta_2+\pi\eta_2+\eta_1\eta_2)}$$

and

$$\frac{\partial^2 f}{\partial S^2}=0 \tag{26}$$

The section shows that at $E_{S0000}(\frac{s_1(\tau+\eta_1)(\tau+\eta_2)}{\tau(\tau^2+\tau t+\tau\eta_1+\pi\eta_1+\tau\eta_2+\pi\eta_2+\eta_1\eta_2)},0,0,0,0)$ period-doubling division of the numerical scheme does not exist. If the period-doubling division is absent, derived variable limitations (20) counteract the non-degeneracy scenario. $(\vartheta,\gamma_1,\tau,\pi,\vartheta_2,\gamma_2,\beta_1,\beta_2)\in F|_{ES0000(\frac{s_1(\tau+\eta_1)(\tau+\eta_2)}{\tau(\tau^2+\tau t+\tau\eta_1+\pi\eta_1+\tau\eta_2+\pi\eta_2+\eta_1\eta_2)},0,0,0,0)}$. Framework (3) exhibits

period-doubling bifurcation at the next numerical value, as demonstrated by the previously described calculation;

$$T_1(S,V,I_1,I_2,R) = \begin{cases} S \to \frac{s_1(\tau+\eta_1)(\tau+\eta_2)}{\tau(\tau^2+\tau t+\tau\eta_1+\pi\eta_1+\tau\eta_2+\pi\eta_2+\eta_1\eta_2)}, \\ V \to \frac{\pi s_1(\tau+\eta_1)}{\tau(\tau^2+\tau t+\tau\eta_1+\pi\eta_1+\tau\eta_2+\pi\eta_2+\eta_1\eta_2)}, \\ I_1 \to 0, \\ I_2 \to 0, \\ R \to \frac{\pi s_1\eta_2}{\tau(\tau^2+\tau t+\tau\eta_1+\pi\eta_1+\tau\eta_2+\pi\eta_2+\eta_1\eta_2)}. \end{cases}$$

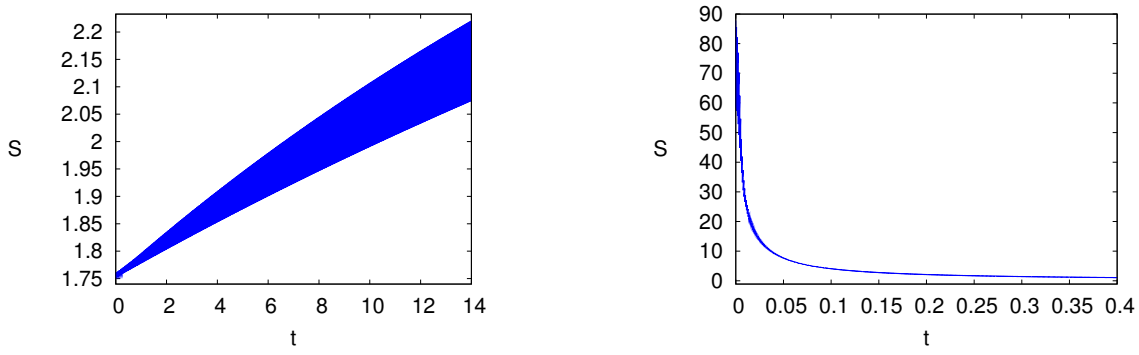

(a) $S(t)$ vs s_1 **(b)** $S(t)$ vs γ_1

Fig. 2: Parameter based bifurcation

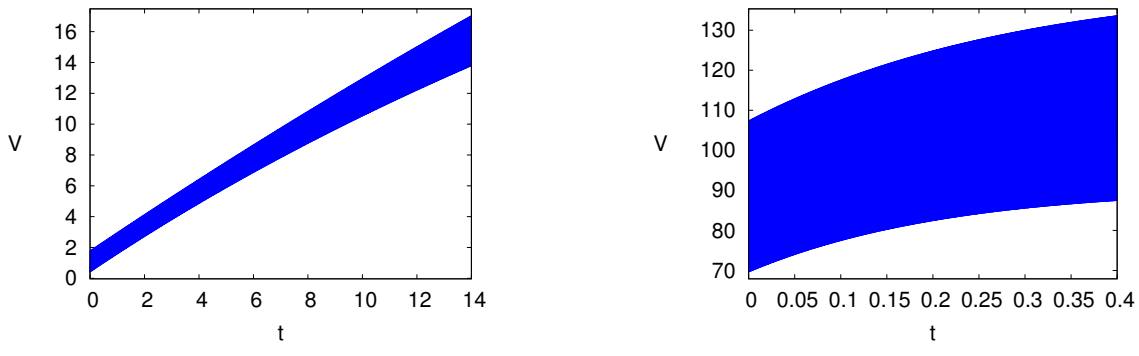

(a) $V(t)$ vs π_1 **(b)** $V(t)$ vs η_2

Fig. 3: Parameter based bifurcation

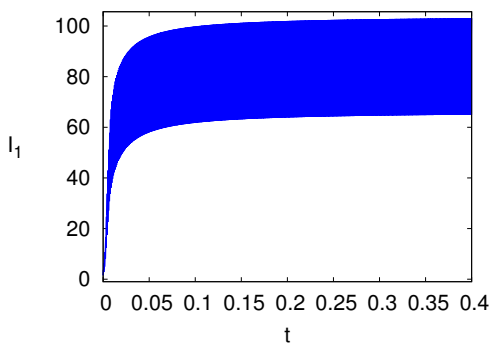

(a) $I_1(t)$ vs γ_1

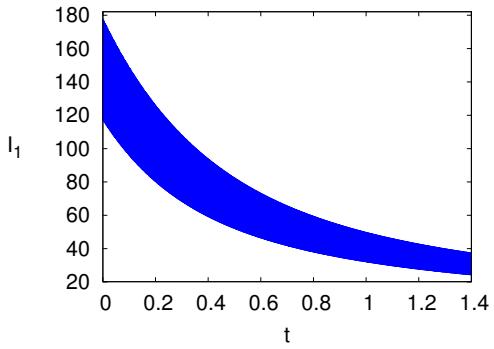

(b) $I_1(t)$ vs γ_2

Fig. 4: Parameter based bifurcation

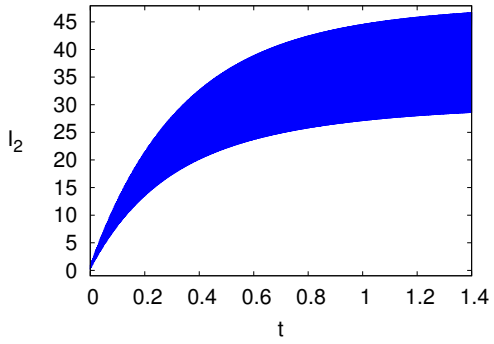

(a) $I_2(t)$ vs γ_2

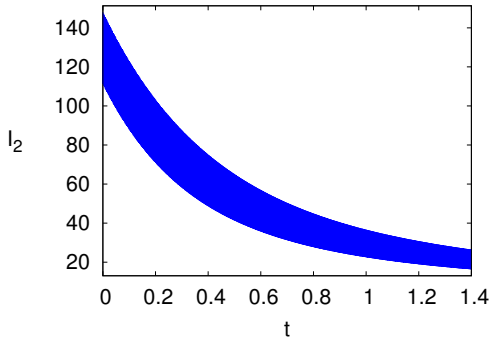

(b) $I_2(t)$ vs β_2

Fig. 5: Parameter based bifurcation

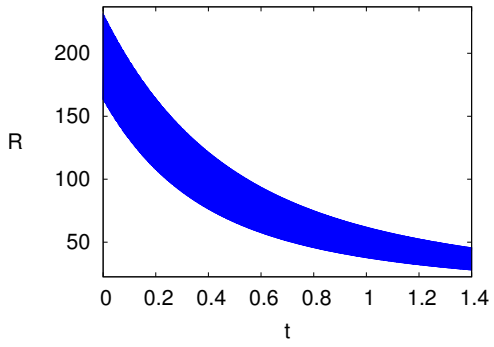

(a) $R(t)$ vs η_1

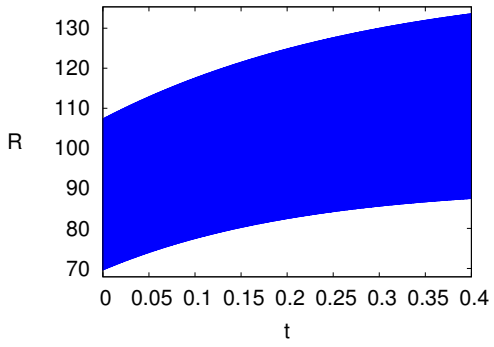

(b) $R(t)$ vs η_2

Fig. 6: Parameter based bifurcation

Figure 2 to figure 6 represents the bifurcation analysis of all compartments under different parameters impacts. It is observed in figure 2 that the susceptible class rises with the parameter s_1, the recruitment rates of the cats, while decreases due to infected rate γ_1 that meets our objectives. Also the primary infected class reduces with the rate from first infection to second infected γ_2 as can be observed in figure 3. Similarly all other compartment impacts can be observed in figure 4, figure 5 and figure 6 according to desired domain and objectives. So, it is deduced that in all compartment there is no bifurcation in it and results must need to approach according to study sate.

5 Numerical Scheme

In the next part, we use the Atangana-Toukfik technique to develop a novel numerical scheme for nonlinear fractional differential equations (SVI_1I_2R) with non-local and non-singular kernels. We will use a non linear fractional differential equation as an example to demonstrate this approach.

$$
\begin{aligned}
{}_0^{ABC}DS(t) &= f_1(t,S,V,I_1,I_2,R),\\
{}_0^{ABC}DV(t) &= f_2(t,S,V,I_1,I_2,R),\\
{}_0^{ABC}DI_1(t) &= f_3(t,S,V,I_1,I_2,R),\\
{}_0^{ABC}DI_2(t) &= f_4(t,S,V,I_1,I_2,R),\\
{}_0^{ABC}DR(t) &= f_5(t,S,V,I_1,I_2,R).
\end{aligned}
$$

Considering the starting circumstances $S(0)=S^{\circ},V(0)=V^{\circ},I_1(0)=I_1^{\circ},I_2(0)=I_2^{\circ},R(0)=R^{\circ}$. The aforementioned system of equation*s is transformed into the relevant fractional fractal integral forms using the fundamental theorem of fractional calculus.

$$
\begin{aligned}
S(t)-S(0) &= \frac{1-\mu}{ABC(\mu)}f_1(t,,S,V,I_1,I_2,R)+\frac{\mu}{ABC(\mu)\Gamma(\mu)}\int_0^1 f_1(\mu,S(\mu),V(\mu),I_1(\mu),I_2(\mu),R(\mu))(t-\mu)^{\mu-1}d\mu,\\
V(t)-V(0) &= \frac{1-\mu}{ABC(\mu)}f_2(t,,S,V,I_1,I_2,R)+\frac{\mu}{ABC(\mu)\Gamma(\mu)}\int_0^1 f_2(\mu,S(\mu),V(\mu),I_1(\mu),I_2(\mu),R(\mu))(t-\mu)^{\mu-1}d\mu,\\
I_1(t)-I_1(0) &= \frac{1-\mu}{ABC(\mu)}f_3(t,,S,V,I_1,I_2,R)+\frac{\mu}{ABC(\mu)\Gamma(\mu)}\int_0^1 f_3(\mu,S(\mu),V(\mu),I_1(\mu),I_2(\mu),R(\mu))(t-\mu)^{\mu-1}d\mu,\\
I_2(t)-I_2(0) &= \frac{1-\mu}{ABC(\mu)}f_4(t,,S,V,I_1,I_2,R)+\frac{\mu}{ABC(\mu)\Gamma(\mu)}\int_0^1 f_4(\mu,S(\mu),V(\mu),I_1(\mu),I_2(\mu),R(\mu))(t-\mu)^{\mu-1}d\mu,\\
R(t)-R(0) &= \frac{1-\mu}{ABC(\mu)}f_5(t,,S,V,I_1,I_2,R)+\frac{\mu}{ABC(\mu)\Gamma(\mu)}\int_0^1 f_5(\mu,S(\mu),V(\mu),I_1(\mu),I_2(\mu),R(\mu))(t-\mu)^{\mu-1}d\mu.
\end{aligned}
$$

At the distinct moments when t = t_{n+1}, n = 0,1,2,3,4..., the preceding equation* can be reformulated as;

$$
\begin{aligned}
S(t_{c+1})-S(0) &= \frac{1-\mu}{ABC(\mu)}f_1(t_c,S(t_c),V(t_c),I_1(t_c),I_2(t_c),R(t_c))+\frac{\mu}{ABC(\mu)\Gamma(\mu)}\\
&\int_0^{t_{c+1}} f_1(\mu,S(\mu),V(\mu),I_1(\mu),I_2(\mu),R(\mu))(t_{c+1}-\mu)^{\mu-1}d\mu,\\
S(t_{c+1})-S(0) &= \frac{1-\mu}{ABC(\mu)}f_1(t_c,S(t_c),V(t_c),I_1(t_c),I_2(t_c),R(t_c))+\frac{\mu}{ABC(\mu)\Gamma(\mu)}\\
&\sum_{l=0}^{c}\int_0^{t_{c+1}} f_1(\mu,S(\mu),V(\mu),I_1(\mu),I_2(\mu),R(\mu))(t_{c+1}-\mu)^{\mu-1}d\mu,\\
V(t_{c+1})-V(0) &= \frac{1-\mu}{ABC(\mu)}f_2(t_c,S(t_c),V(t_c),I_1(t_c),I_2(t_c),R(t_c))+\frac{\mu}{ABC(\mu)\Gamma(\mu)}\\
&\int_0^{t_{c+1}} f_2(\mu,S(\mu),V(\mu),I_1(\mu),I_2(\mu),R(\mu))(t_{c+1}-\mu)^{\mu-1}d\mu,
\end{aligned}
$$

$$V(t_{c+1})-V(0)=\frac{1-\mu}{ABC(\mu)}f_2(t_c,S(t_c),V(t_c),I_1(t_c),I_2(t_c),R(t_c))+\frac{\mu}{ABC(\mu)\Gamma(\mu)}$$
$$\sum_{l=0}^{c}\int_0^{t_{c+1}}f_2(\mu,S(\mu),V(\mu),I_1(\mu),I_2(\mu),R(\mu))(t_{c+1}-\mu)^{\mu-1}d\mu,$$

$$I_1(t_{c+1})-I_1(0)=\frac{1-\mu}{ABC(\mu)}f_3(t_c,S(t_c),V(t_c),I_1(t_c),I_2(t_c),R(t_c))+\frac{\mu}{ABC(\mu)\Gamma(\mu)}$$
$$\int_0^{t_{c+1}}f_3(\mu,S(\mu),V(\mu),I_1(\mu),I_2(\mu),R(\mu))(t_{c+1}-\mu)^{\mu-1}d\mu,$$

$$I_1(t_{c+1})-I_1(0)=\frac{1-\mu}{ABC(\mu)}f_3(t_c,S(t_c),V(t_c),I_1(t_c),I_2(t_c),R(t_c))+\frac{\mu}{ABC(\mu)\Gamma(\mu)}$$
$$\sum_{l=0}^{c}\int_0^{t_{c+1}}f_3(\mu,S(\mu),V(\mu),I_1(\mu),I_2(\mu),R(\mu))(t_{c+1}-\mu)^{\mu-1}d\mu,$$

$$I_2(t_{c+1})-I_2(0)=\frac{1-\mu}{ABC(\mu)}f_4(t_c,S(t_c),V(t_c),I_1(t_c),I_2(t_c),R(t_c))+\frac{\mu}{ABC(\mu)\Gamma(\mu)}$$
$$\int_0^{t_{c+1}}f_4(\mu,S(\mu),V(\mu),I_1(\mu),I_2(\mu),R(\mu))(t_{c+1}-\mu)^{\mu-1}d\mu,$$

$$I_2(t_{c+1})-I_2(0)=\frac{1-\mu}{ABC(\mu)}f_4(t_c,S(t_c),V(t_c),I_1(t_c),I_2(t_c),R(t_c))+\frac{\mu}{ABC(\mu)\Gamma(\mu)}$$
$$\sum_{l=0}^{c}\int_0^{t_{c+1}}f_4(\mu,S(\mu),V(\mu),I_1(\mu),I_2(\mu),R(\mu))(t_{c+1}-\mu)^{\mu-1}d\mu,$$

$$R(t_{c+1})-R(0)=\frac{1-\mu}{ABC(\mu)}f_5(t_c,S(t_c),V(t_c),I_1(t_c),I_2(t_c),R(t_c))+\frac{\mu}{ABC(\mu)\Gamma(\mu)}$$
$$\int_0^{t_{c+1}}f_5(\mu,S(\mu),V(\mu),I_1(\mu),I_2(\mu),R(\mu))(t_{c+1}-\mu)^{\mu-1}d\mu,$$

$$R(t_{c+1})-R(0)=\frac{1-\mu}{ABC(\mu)}f_5(t_c,S(t_c),V(t_c),I_1(t_c),I_2(t_c),R(t_c))+\frac{\mu}{ABC(\mu)\Gamma(\mu)}$$
$$\sum_{l=0}^{c}\int_0^{t_{c+1}}f_5(\mu,S(\mu),V(\mu),I_1(\mu),I_2(\mu),R(\mu))(t_{c+1}-\mu)^{\mu-1}d\mu.$$

Across the span of the interval $[t_\vartheta,t_{\vartheta+1}]$ the expression $f_1(\mu,S(\mu),V(\mu),I_1(\mu),I_2(\mu),R(\mu))$. In order to estimate and constrain the results inside the interval's bounds, we will now use a two-phase Lagrange polynomial interpolation approach $[t_\vartheta,t_{\vartheta+1}]$, the expression $f_1(\mu,S(\mu),V(\mu),I_1(\mu),I_2(\mu),R(\mu))$. We will now use a two-step Lagrange polynomial estimate method, which is expressed as follows:

$$Q_\vartheta(\mu)=\frac{\mu-t_\vartheta-1}{t_\vartheta-t_\vartheta-1}f_1(t_\vartheta,S(t_\vartheta),V(t_\vartheta),I_1(t_\vartheta),I_2(t_\vartheta),R(t_\vartheta))-\frac{Q-t_\vartheta}{t_\vartheta-t_\vartheta-1}f_1(t_{\vartheta-1},S(t_{\vartheta-1}),V(t_{\vartheta-1}),I_1(t_{\vartheta-1}),I_2(t_{\vartheta-1}),R(t_{\vartheta-1})),$$

$$Q_\vartheta(\mu)=\frac{f_1(t_\vartheta,S(t_\vartheta),V(t_\vartheta),I_1(t_\vartheta),I_2(t_\vartheta),R(t_\vartheta))}{h}(\mu-t_{\vartheta-1})-\frac{f_1(t_{\vartheta-1},S(t_{\vartheta-1}),V(t_{\vartheta-1}),I_1(t_{\vartheta-1}),I_2(t_{\vartheta-1}),R(t_{\vartheta-1}))}{h}(\mu-t_\vartheta)$$
$$\approx\frac{f_1(t_\vartheta,S(t_\vartheta),V(t_\vartheta),I_1(t_\vartheta),I_2(t_\vartheta),R(t_\vartheta))}{h}(\mu-t_{\vartheta-1})-\frac{f_1(t_{\vartheta-1},S(t_{\vartheta-1}),V(t_{\vartheta-1}),I_1(t_{\vartheta-1}),I_2(t_{\vartheta-1}),R(t_{\vartheta-1}))}{h}(\mu-t_\vartheta).$$

Within the bounds of interval $[t_\vartheta,t_{\vartheta+1}]$ the function $f_2(\mu,S(\mu),V(\mu),I_1(\mu),I_2(\mu),R(\mu))$. Next we use Lagrange polynomial interpolation, which may be roughly represented as follows, to implement the two-step method;

$$Q_\vartheta(\mu)=\frac{\mu-t_\vartheta-1}{t_\vartheta-t_\vartheta-1}f_2(t_\vartheta,S(t_\vartheta),V(t_\vartheta),I_1(t_\vartheta),I_2(t_\vartheta),R(t_\vartheta))-\frac{Q-t_\vartheta}{t_\vartheta-t_\vartheta-1}f_2(t_{\vartheta-1},S(t_{\vartheta-1}),V(t_{\vartheta-1}),I_1(t_{\vartheta-1}),I_2(t_{\vartheta-1}),R(t_{\vartheta-1})),$$

$$Q_\vartheta(\mu)=\frac{f_2(t_\vartheta,S(t_\vartheta),V(t_\vartheta),I_1(t_\vartheta),I_2(t_\vartheta),R(t_\vartheta))}{h}(\mu-t_{\vartheta-1})-\frac{f_2(t_{\vartheta-1},S(t_{\vartheta-1}),V(t_{\vartheta-1}),I_1(t_{\vartheta-1}),I_2(t_{\vartheta-1}),R(t_{\vartheta-1}))}{h}(\mu-t_\vartheta)$$

$$\approx \frac{f_2(t_\vartheta,S(t_\vartheta),V(t_\vartheta),I_1(t_\vartheta),I_2(t_\vartheta),R(t_\vartheta))}{h}(\mu-t_{\vartheta-1})-\frac{f_2(t_{\vartheta-1},S(t_{\vartheta-1}),V(t_{\vartheta-1}),I_1(t_{\vartheta-1}),I_2(t_{\vartheta-1}),R(t_{\vartheta-1}))}{h}(\mu-t_\vartheta).$$

Within the bounds of interval $[t_\vartheta,t_{\vartheta+1}]$ the function $f_3(\mu,S(\mu),V(\mu),I_1(\mu),I_2(\mu),R(\mu))$. Now we use a two-step process that is based on Lagrange polynomial interpolation, which is roughly represented as follows;

$$Q_\vartheta(\mu)=\frac{\mu-t_\vartheta-1}{t_\vartheta-t_\vartheta-1}f_3(t_\vartheta,S(t_\vartheta),V(t_\vartheta),I_1(t_\vartheta),I_2(t_\vartheta),R(t_\vartheta))-\frac{Q-t_\vartheta}{t_\vartheta-t_\vartheta-1}f_3(t_{\vartheta-1},S(t_{\vartheta-1}),V(t_{\vartheta-1}),I_1(t_{\vartheta-1}),I_2(t_{\vartheta-1}),R(t_{\vartheta-1})),$$

$$Q_\vartheta(\mu)=\frac{f_3(t_\vartheta,S(t_\vartheta),V(t_\vartheta),I_1(t_\vartheta),I_2(t_\vartheta),R(t_\vartheta))}{h}(\mu-t_{\vartheta-1})-\frac{f_3(t_{\vartheta-1},S(t_{\vartheta-1}),V(t_{\vartheta-1}),I_1(t_{\vartheta-1}),I_2(t_{\vartheta-1}),R(t_{\vartheta-1}))}{h}(\mu-t_\vartheta)$$

$$\approx \frac{f_3(t_\vartheta,S(t_\vartheta),V(t_\vartheta),I_1(t_\vartheta),I_2(t_\vartheta),R(t_\vartheta))}{h}(\mu-t_{\vartheta-1})-\frac{f_3(t_{\vartheta-1},S(t_{\vartheta-1}),V(t_{\vartheta-1}),I_1(t_{\vartheta-1}),I_2(t_{\vartheta-1}),R(t_{\vartheta-1}))}{h}(\mu-t_\vartheta).$$

Within the bounds of interval $[t_\vartheta,t_{\vartheta+1}]$ the function $f_4(\mu,S(\mu),V(\mu),I_1(\mu),I_2(\mu),R(\mu))$. The two-step Lagrange polynomial interpolation approach, which may be roughly described as follows;

$$Q_\vartheta(\mu)=\frac{\mu-t_\vartheta-1}{t_\vartheta-t_\vartheta-1}f_4(t_\vartheta,S(t_\vartheta),V(t_\vartheta),I_1(t_\vartheta),I_2(t_\vartheta),R(t_\vartheta))-\frac{Q-t_\vartheta}{t_\vartheta-t_\vartheta-1}f_4(t_{\vartheta-1},S(t_{\vartheta-1}),V(t_{\vartheta-1}),I_1(t_{\vartheta-1}),I_2(t_{\vartheta-1}),R(t_{\vartheta-1})),$$

$$Q_\vartheta(\mu)=\frac{f_4(t_\vartheta,S(t_\vartheta),V(t_\vartheta),I_1(t_\vartheta),I_2(t_\vartheta),R(t_\vartheta))}{h}(\mu-t_{\vartheta-1})-\frac{f_4(t_{\vartheta-1},S(t_{\vartheta-1}),V(t_{\vartheta-1}),I_1(t_{\vartheta-1}),I_2(t_{\vartheta-1}),R(t_{\vartheta-1}))}{h}(\mu-t_\vartheta)$$

$$\approx \frac{f_4(t_\vartheta,S(t_\vartheta),V(t_\vartheta),I_1(t_\vartheta),I_2(t_\vartheta),R(t_\vartheta))}{h}(\mu-t_{\vartheta-1})-\frac{f_4(t_{\vartheta-1},S(t_{\vartheta-1}),V(t_{\vartheta-1}),I_1(t_{\vartheta-1}),I_2(t_{\vartheta-1}),R(t_{\vartheta-1}))}{h}(\mu-t_\vartheta).$$

Within the bounds of interval $[t_\vartheta,t_{\vartheta+1}]$ the function $f_5(\mu,S(\mu),V(\mu),I_1(\mu),I_2(\mu),R(\mu))$.

$$Q_\vartheta(\mu)=\frac{\mu-t_\vartheta-1}{t_\vartheta-t_\vartheta-1}f_5(t_\vartheta,S(t_\vartheta),V(t_\vartheta),I_1(t_\vartheta),I_2(t_\vartheta),R(t_\vartheta))-\frac{Q-t_\vartheta}{t_\vartheta-t_\vartheta-1}f_5(t_{\vartheta-1},S(t_{\vartheta-1}),V(t_{\vartheta-1}),I_1(t_{\vartheta-1}),I_2(t_{\vartheta-1}),R(t_{\vartheta-1})),$$

$$Q_\vartheta(\mu)=\frac{f_5(t_\vartheta,S(t_\vartheta),V(t_\vartheta),I_1(t_\vartheta),I_2(t_\vartheta),R(t_\vartheta))}{h}(\mu-t_{\vartheta-1})-\frac{f_5(t_{\vartheta-1},S(t_{\vartheta-1}),V(t_{\vartheta-1}),I_1(t_{\vartheta-1}),I_2(t_{\vartheta-1}),R(t_{\vartheta-1}))}{h}(\mu-t_\vartheta)$$

$$\approx \frac{f_5(t_\vartheta,S(t_\vartheta),V(t_\vartheta),I_1(t_\vartheta),I_2(t_\vartheta),R(t_\vartheta))}{h}(\mu-t_{\vartheta-1})-\frac{f_5(t_{\vartheta-1},S(t_{\vartheta-1}),V(t_{\vartheta-1}),I_1(t_{\vartheta-1}),I_2(t_{\vartheta-1}),R(t_{\vartheta-1}))}{h}(\mu-t_\vartheta).$$

Since our goal is to prove the validity of this approximation, we include it in the equation*;

$$S_{c+1}=S_0+\frac{1-\mu}{ABC(\mu)}f_1(t_c,S(t_c),V(t_c),I_1(t_c),I_2(t_c),R(t_c))+\frac{\mu}{ABC(\mu)\Gamma(\mu)}$$

$$\sum_{\vartheta=0}^{b}\frac{f_1(t_\vartheta,S_\vartheta,V_\vartheta,I_{1\vartheta},I_{2\vartheta}),R_\vartheta}{h}\int_{t_\vartheta}^{t_{\vartheta+1}}(\mu-t_\vartheta-1)(t_{c+1}-\mu)^{\mu-1}d\mu$$

$$-\frac{f_1(t_{\vartheta-1},S_{\vartheta-1},V_{\vartheta-1},I_{1(\vartheta-1)},I_{2(\vartheta-1)},R_{\vartheta-1})}{h}\int_{t_\vartheta}^{t_{\vartheta+1}}(\mu-t_\vartheta-1)(t_{c+1}-\mu)^{\mu-1}d\mu,$$

$$V_{c+1}=V_0+\frac{1-\mu}{ABC(\mu)}f_2(t_c,S(t_c),V(t_c),I_1(t_c),I_2(t_c),R(t_c))+\frac{\mu}{ABC(\mu)\Gamma(\mu)}$$

$$\sum_{\vartheta=0}^{b}\frac{f_2(t_\vartheta,S_\vartheta,V_\vartheta,I_{1\vartheta},I_{2\vartheta}),R_\vartheta}{h}\int_{t_\vartheta}^{t_{\vartheta+1}}(\mu-t_\vartheta-1)(t_{c+1}-\mu)^{\mu-1}d\mu$$

$$-\frac{f_2(t_{\vartheta-1},S_{\vartheta-1},V_{\vartheta-1},I_{1(\vartheta-1)},I_{2(\vartheta-1)},R_{\vartheta-1})}{h}\int_{t_\vartheta}^{t_{\vartheta+1}}(\mu-t_\vartheta-1)(t_{c+1}-\mu)^{\mu-1}d\mu,$$

$$I_{1(c+1)}=I_{1(0)}+\frac{1-\mu}{ABC(\mu)}f_3(t_c,S(t_c),V(t_c),I_1(t_c),I_2(t_c),R(t_c))+\frac{\mu}{ABC(\mu)\Gamma(\mu)}$$

$$\sum_{\vartheta=0}^{b}\frac{f_3(t_\vartheta,S_\vartheta,V_\vartheta,I_{1\vartheta},I_{2\vartheta}),R_\vartheta}{h}\int_{t_\vartheta}^{t_{\vartheta+1}}(\mu-t_\vartheta-1)(t_{c+1}-\mu)^{\mu-1}d\mu$$

$$-\frac{f_3(t_{\vartheta-1},S_{\vartheta-1},V_{\vartheta-1},I_{1(\vartheta-1)},I_{2(\vartheta-1)},R_{\vartheta-1})}{h}\int_{t_\vartheta}^{t_{\vartheta+1}}(\mu-t_\vartheta-1)(t_{c+1}-\mu)^{\mu-1}d\mu,$$

$$I_{2(c+1)}=I_{2(0)}+\frac{1-\mu}{ABC(\mu)}f_4(t_c,S(t_c),V(t_c),I_1(t_c),I_2(t_c),R(t_c))+\frac{\mu}{ABC(\mu)\Gamma(\mu)}$$

$$\sum_{\vartheta=0}^{b}\frac{f_4(t_\vartheta,S_\vartheta,V_\vartheta,I_{1\vartheta},I_{2\vartheta}),R_\vartheta}{h}\int_{t_\vartheta}^{t_{\vartheta+1}}(\mu-t_\vartheta-1)(t_{c+1}-\mu)^{\mu-1}d\mu$$

$$-\frac{f_4(t_{\vartheta-1},S_{\vartheta-1},V_{\vartheta-1},I_{1(\vartheta-1)},I_{2(\vartheta-1)},R_{\vartheta-1})}{h}\int_{t_\vartheta}^{t_{\vartheta+1}}(\mu-t_\vartheta-1)(t_{c+1}-\mu)^{\mu-1}d\mu,$$

$$R_{c+1}=R_0+\frac{1-\mu}{ABC(\mu)}f_5(t_c,S(t_c),V(t_c),I_1(t_c),I_2(t_c),R(t_c))+\frac{\mu}{ABC(\mu)\Gamma(\mu)}$$

$$\sum_{\vartheta=0}^{b}\frac{f_5(t_\vartheta,S_\vartheta,V_\vartheta,I_{1\vartheta},I_{2\vartheta}),R_\vartheta}{h}\int_{t_\vartheta}^{t_{\vartheta+1}}(\mu-t_\vartheta-1)(t_{c+1}-\mu)^{\mu-1}d\mu$$

$$-\frac{f_5(t_{\vartheta-1},S_{\vartheta-1},V_{\vartheta-1},I_{1(\vartheta-1)},I_{2(\vartheta-1)},R_{\vartheta-1})}{h}\int_{t_\vartheta}^{t_{\vartheta+1}}(\mu-t_\vartheta-1)(t_{c+1}-\mu)^{\mu-1}d\mu,$$

We rewrite it as simply as possible. Let's clarify;

$$F_{\mu,\vartheta,1}=\int_{t_\vartheta}^{t_{\vartheta+1}}(\mu-t_\vartheta-1)(t_{c+1}-\mu),$$

$$F_{\mu,\vartheta,2}=\int_{t_\vartheta}^{t_{\vartheta+1}}(\mu-t_\vartheta-1)(t_{c+1}-\mu).$$

The integration of the equation*s is then carried out;

$$S_{c+1}=S_0+\frac{(1-\mu)}{ABC(\mu)}f_1(t_c,S(t_c),V(t_c),I_1(t_c),I_2(t_c),R(t_c))+\frac{\mu}{ABC(\mu)}$$

$$\sum_{\vartheta=0}^{B}\frac{h^\mu f_1(t_\vartheta,S_\vartheta,V_\vartheta,I_{1\vartheta},I_{2\vartheta},R_\vartheta)}{\Gamma(\mu+2)}((b+1-\vartheta)^\mu(b-\vartheta+2+\mu)-(b-\vartheta)\mu(b-\vartheta+2+2\mu))$$

$$-\frac{h^\mu f_1(t_{\vartheta-1},S_{\vartheta-1},V_{\vartheta-1},I_{1(\vartheta-1)},I_{2(\vartheta-1)},R_{\vartheta-1})}{\Gamma(\mu+2)}((b+1-\vartheta)^{\mu-1}-(b-\vartheta)^\mu(b-\vartheta+1+\mu)),$$

$$V_{c+1}=V_0+\frac{(1-\mu)}{ABC(\mu)}f_2(t_c,S(t_c),V(t_c),I_1(t_c),I_2(t_c),R(t_c))+\frac{\mu}{ABC(\mu)}$$

$$\sum_{\vartheta=0}^{B}\frac{h^\mu f_2(t_\vartheta,S_\vartheta,V_\vartheta,I_{1\vartheta},I_{2\vartheta},R_\vartheta)}{\Gamma(\mu+2)}((b+1-\vartheta)^\mu(b-\vartheta+2+\mu)-(b-\vartheta)\mu(b-\vartheta+2+2\mu))$$

$$-\frac{h^\mu f_2(t_{\vartheta-1},S_{\vartheta-1},V_{\vartheta-1},I_{1(\vartheta-1)},I_{2(\vartheta-1)},R_{(\vartheta-1)})}{\Gamma(\mu+2)}((b+1-\vartheta)^{\mu-1}-(b-\vartheta)^\mu(b-\vartheta+1+\mu)),$$

$$I_{1(c+1)}=S_{1(0)}+\frac{(1-\mu)}{ABC(\mu)}f_3(t_c,S(t_c),V(t_c),I_1(t_c),I_2(t_c),R(t_c))+\frac{\mu}{ABC(\mu)}$$

$$\sum_{\vartheta=0}^{B}\frac{h^\mu f_3(t_\vartheta,S_\vartheta,V_\vartheta,I_{1\vartheta},I_{2\vartheta},R_\vartheta)}{\Gamma(\mu+2)}((b+1-\vartheta)^\mu(b-\vartheta+2+\mu)-(b-\vartheta)\mu(b-\vartheta+2+2\mu))$$

$$-\frac{h^\mu f_3(t_{\vartheta-1},S_{\vartheta-1},V_{\vartheta-1},I_{1(\vartheta-1)},I_{2(\vartheta-1)},R_{(\vartheta-1)})}{\Gamma(\mu+2)}((b+1-\vartheta)^{\mu-1}-(b-\vartheta)^\mu(b-\vartheta+1+\mu)),$$

$$I_{2(c+1)}=I_{2(0)}+\frac{(1-\mu)}{ABC(\mu)}f_4(t_c,S(t_c),V(t_c),I_1(t_c),I_2(t_c),R(t_c))+\frac{\mu}{ABC(\mu)}$$

$$\sum_{\vartheta=0}^{B}\frac{h^{\mu}f_4(t_\vartheta,S_\vartheta,V_\vartheta,I_{1\vartheta},I_{2\vartheta},R_\vartheta)}{\Gamma(\mu+2)}((b+1-\vartheta)^{\mu}(b-\vartheta+2+\mu)-(b-\vartheta)\mu(b-\vartheta+2+2\mu))$$

$$-\frac{h^{\mu}f_4(t_{\vartheta-1},S_{\vartheta-1},V_{\vartheta-1},I_{1(\vartheta-1)},I_{2(\vartheta-1)},R_{(\vartheta-1)})}{\Gamma(\mu+2)}((b+1-\vartheta)^{\mu-1}-(b-\vartheta)^{\mu}(b-\vartheta+1+\mu)),$$

$$R_{c+1}=R_0+\frac{(1-\mu)}{ABC(\mu)}f_5(t_c,S(t_c),V(t_c),I_1(t_c),I_2(t_c),R(t_c))+\frac{\mu}{ABC(\mu)}.$$

$$\sum_{\vartheta=0}^{B}\frac{h^{\mu}f_5(t_\vartheta,S_\vartheta,V_\vartheta,I_{1\vartheta},I_{2\vartheta},R_\vartheta)}{\Gamma(\mu+2)}((b+1-\vartheta)^{\mu}(b-\vartheta+2+\mu)-(b-\vartheta)\mu(b-\vartheta+2+2\mu))$$

$$-\frac{h^{\mu}f_5(t_{\vartheta-1},S_{\vartheta-1},V_{\vartheta-1},I_{1(\vartheta-1)},I_{2(\vartheta-1)},R_{(\vartheta-1)})}{\Gamma(\mu+2)}((b+1-\vartheta)^{\mu-1}-(b-\vartheta)^{\mu}(b-\vartheta+1+\mu)),$$

6 Physical interpretation

In this work, we derived theoretical insights and applied an advanced computational technique to assess their accuracy for the newly established SVI_1I_2R framework. This framework characterizes the interaction and transmission of Toxoplasma gondii between the cat population and the environment. The ABC fractional derivative technique was employed to model the system, incorporating memory effects and non-local dynamics, while deterministic fluctuations and a generalized incidence rate provided a more realistic depiction of parasite transmission. By integrating the influence of vaccination and environmental sanitation into this fractional-order model, we achieved consistent and meaningful outcomes. MATLAB-based numerical simulations of the SVI_1I_2R system were carried out using the parameter values $s_1 = .89$, $\vartheta_1 = 0.3$, $\gamma_1 = 0.23$, $\gamma_2 = 0.34$, $\tau = 0.43$, $\pi = 0.613$, $\vartheta_2 = 0.98$, $\beta_1 = 0.123$ and $\beta_2 = 0.97$ to validate the analytical observations and confirm the logical conclusions. The graphical results illustrate the temporal evolution of the susceptible (S), vaccinated (V), primary infected (I_1), secondary infected (I_2), and recovered (R) compartments under different fractional orders, as shown in Figures 7, 8, 9, 10 and 11 respectively. It is observed that the susceptible (S), vaccinated (V) and recovered (R) class rises with the passage of time due to rise in vaccination and early identification and faster converge to steady state by reducing the fractional values as can be seen in figure 7, figure 8 and figure 11 respectively. Similarly the both infected classes primary infected (I_1) and secondary infected (I_2) reduces due according to the designed objectives and model formulations and can be seen in figure 9 and figure 11 respectively. Similar behavior can be seen in all compartment by reducing the dimensions with minor effects but it give better convergence by reducing dimensions from 0.8 to 0.5. The findings reveal an early increase in infection levels that gradually decreases and stabilizes over time. Crucially, the model demonstrates that strengthened vaccination strategies and improved sanitation measures markedly reduce both environmental contamination and infection prevalence including early identification. Furthermore, the model delivers precise and dependable outcomes across various fractional derivative levels, confirming that smaller fractional parameters contribute to improved model stability and biological realism. Ultimately, this advanced numerical framework outlines effective intervention policies and refined control techniques to curb the spread of Toxoplasma gondii.

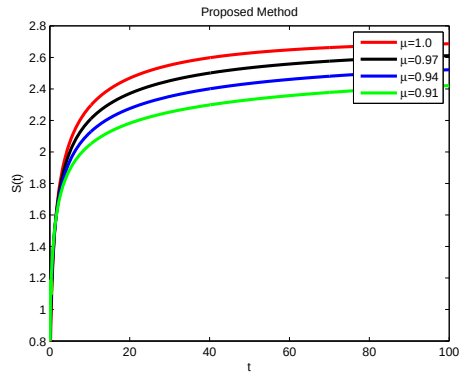

(a) S(t) under dimension 0.5

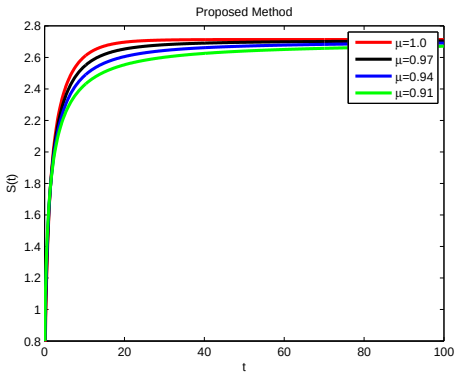

(b) S(t) under dimension 0.8

Fig. 7: Simulation of S(t)

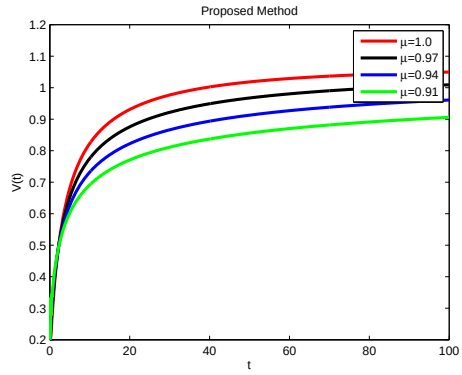

(a) V(t) under dimension 0.5

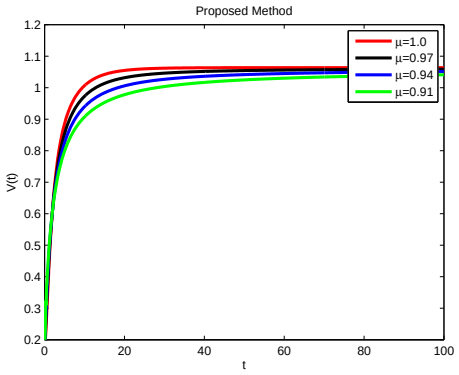

(b) V(t) under dimension 0.8

Fig. 8: Simulation of V(t)

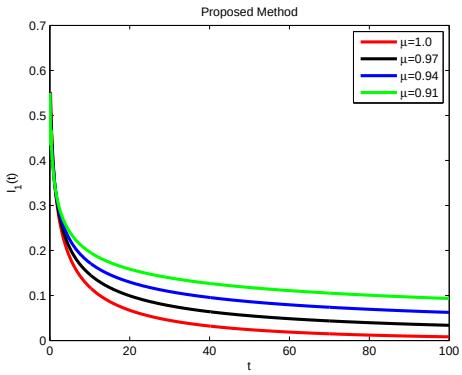

(a) $I_1(t)$ under dimension 0.5

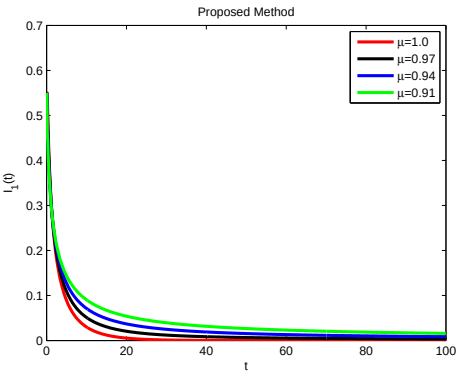

(b) $I_1(t)$ under dimension 0.8

Fig. 9: Simulation of $I_1(t)$

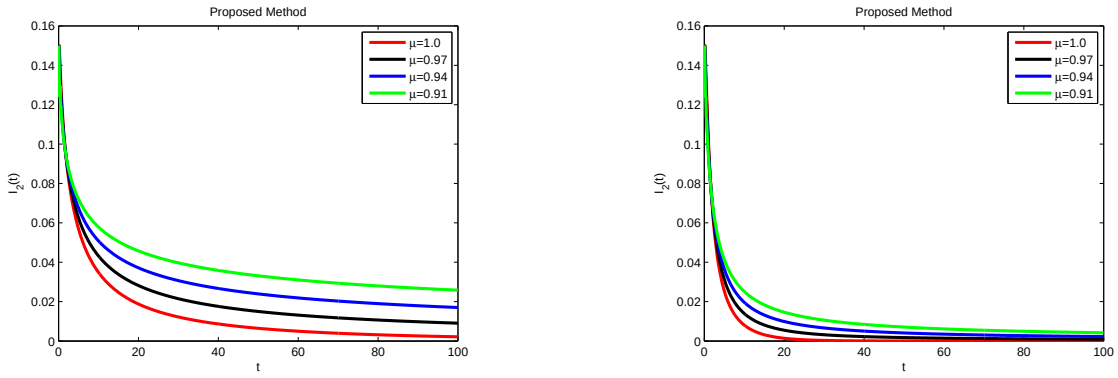

(a) $I_2(t)$ under dimension 0.5 **(b)** $I_2(t)$ under dimension 0.8

Fig. 10: Simulation of $I_2(t)$

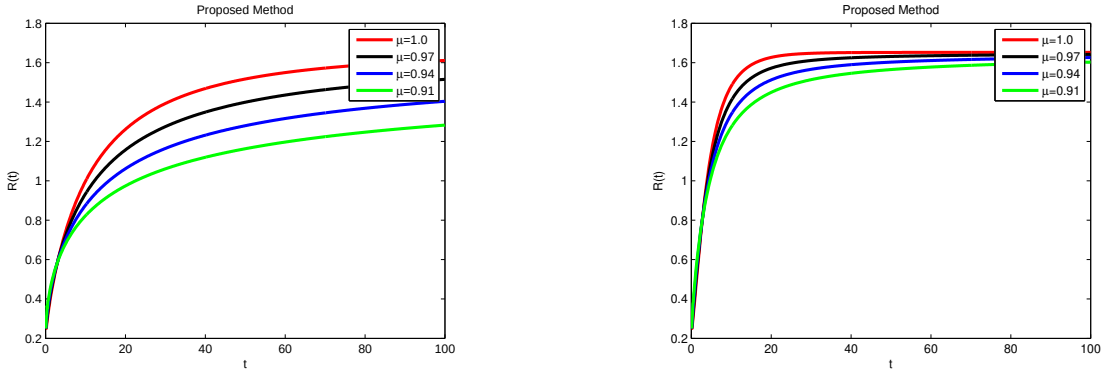

(a) R(t) under dimension 0.5 **(b)** R(t) under dimension 0.5

Fig. 11: Simulation of R(t)

7 Conclusions

We created a general mathematical framework with a more realistic structure to study the transmission dynamics of toxoplasmosis. The model incorporates two distinct effects of vaccination and sanitation, also the first represents the time a susceptible cat must wait to become infectious after being exposed to oocysts, and the second represents the time elapsed between the release of oocysts into the environment and the point at which they can infect a host. Finding the circumstances under which toxoplasmosis may be eliminated from the cat population possible only in the absence of environmental oocysts is a significant contribution of this work. On the other hand, we created scenarios where the illness continues to spread and becomes endemic. The research demonstrates that a stable endemic equilibrium is established including qualitative and quantitative analysis. Also verify that bifurcation does not exist with different parameters impacts. The developed solution represented by simulation to see the actual behavior. The findings under complete analysis including simulation provide a framework for evaluating the effectiveness of immunization campaigns for cats based on more grounded hypotheses with vaccination. The suggested model might be fitted to empirical facts if there were enough information on state variables, such as the density of oocysts or the percentage of diseased cats. Although a thorough identifiability investigation would be necessary to determine whether this calibration is unique, it is possible because approximations of values for some parameters are available. Although some unanswered questions remain overall, this study enhances our understanding of the dynamics of toxoplasmosis. For example, adding more hosts to the model, such as rats, would capture crucial elements of the transmission cycle, which is a research constraint.

There will always be simplifications, as with any mathematical depiction of biological processes. Even if they are more complicated, future studies that include intermediate hosts or further delays may improve the realism and usefulness of these models even more and can be implemented on the real data.

References

[1] M. Attias, D. E. Teixeira, M. Benchimol, R. C. Vommaro, P. H. Crepaldi, and W. De Souza, "The life-cycle of Toxoplasma gondii reviewed using animations," Parasit Vectors, vol. 13, no. 1, p. 588, Dec. 2020.

[2] J. P. Dubey, "Outbreaks of clinical toxoplasmosis in humans: five decades of personal experience, perspectives and lessons learned," Parasit Vectors, vol. 14, no. 1, p. 263, Jun. 2021.

[3] J. P. Dubey, "History of the discovery of the life cycle of Toxoplasma gondii," Int. J. Parasitol., vol. 39, no. 8, pp. 877-882, Jul. 2009.

[4] A. J. C. Gonzalez, I. V. Matos, and V. M. Revoredo, "Acute toxoplasmosis complicated with myopericarditis and possible encephalitis in an immunocompetent patient," IDCases, vol. 20, 2020.

[5] C. Alvarado-Esquivel et al., "Toxoplasma gondii infection and insomnia: A case control seroprevalence study," PLoS ONE, vol. 17, no. 6, Jun. 2022.

[6] S. Caldrer, A. Vola, G. Ferrari, T. Ursini, C. Mazzi, V. Meroni, and A. Beltrame, "Toxoplasma gondii Serotypes in Italian and Foreign Populations: A Cross-Sectional Study Using a Homemade ELISA Test," Microorg., vol. 10, no. 8, p. 1577, Aug. 2022.

[7] D. A. Almashhadany, A. A. J. Alani, A. A. Dhiab, M. A. M. Zainel, and T. T. Abdulrahman, "Public Health Significance of Human Toxoplasmosis," Preprints, 2024. [Online]. Available: https://www.preprints.org/manuscript/202401.2346/v1. Accessed: Jun. 15, 2024.

[8] J. P. Dubey, "The history of Toxoplasma gondii the first 100 years," J. Eukaryotic Microbiol., vol. 55, no. 6, pp. 467-475, Nov. 2008.

[9] A. H. Havelaar et al., "World Health Organization global estimates and regional comparisons of the burden of foodborne disease in 2010," PLoS Med., vol. 12, no. 12, Dec. 2015.

[10] M. Opsteegh, T. M. Kortbeek, A. H. Havelaar, and J. W. Van Der Giessen, "Intervention strategies to reduce human Toxoplasma gondii disease burden," Clin. Infect. Dis., vol. 60, no. 1, pp. 101-107, Jan. 2015.

[11] E. Scallan et al., "Foodborne illness acquired in the United States major pathogens," Emerg. Infect. Dis., vol. 17, no. 1, pp. 7-15, Jan. 2011.

[12] M. B. Batz, S. Hoffmann, and J. G. Morris, Jr., "Ranking the disease burden of 14 pathogens in food sources in the United States using attribution data from outbreak investigations and expert elicitation," J. Food Prot., vol. 75, no. 7, pp. 1278-1291, Jul. 2012.

[13] H. Deng et al., "Mathematical modelling of Toxoplasma gondii transmission: A systematic review," Food Waterborne Parasitol., vol. 22, Mar. 2021.

[14] J. J. Aramini, C. Stephen, J. P. Dubey, C. Engelstoft, H. Schwantje, and C. S. Ribble, "Potential contamination of drinking water with Toxoplasma gondii oocysts," Epidemiol. Infect., vol. 122, no. 2, pp. 305-315, Apr. 1999.

[15] R. Fayer, "Toxoplasmosis update and public health implications," Can. Vet. J., vol. 22, no. 11, p. 344, Nov. 1981.

[16] E. A. Innes, C. Hamilton, J. L. Garcia, A. Chryssafidis, and D. Smith, "A one health approach to vaccines against Toxoplasma gondii," Food Waterborne Parasitol., vol. 15, Dec. 2019.

[17] J. P. Dubey, "A review of toxoplasmosis in cattle," Vet. Parasitol., vol. 22, no. 34, pp. 177-202, Dec. 1986

[18] J. P. Dubey, M. E. Mattix, and T. P. Lipscomb, "Lesions of neonatally induced toxoplasmosis in cats," Vet. Pathol., vol. 33, no. 3, pp. 290-295, May 1996.

[19] R. G. Murphy, R. H. Williams, J. M. Hughes, G. Hide, N. J. Ford, and D. J. Oldbury, "The urban house mouse (Mus domesticus) as a reservoir of infection for the human parasite Toxoplasma gondii: an unrecognised public health issue?," Int. J. Environ. Health Res., vol. 18, no. 3, pp. 177-185, Jun. 2008.

[20] A. J. Arenas, g. González-Parra, and R. J. V. Micó, "Modeling toxoplasmosis spread in cat populations under vaccination," Theor. Popul. Biol., vol. 77, no. 4, pp. 227-237, Jun. 2010.

[21] J. D. Ferreira, L. M. Echeverry, and C. A. P. Rincon, "Stability and bifurcation in epidemic models describing the transmission of toxoplasmosis in human and cat populations," Math. Methods Appl. Sci., vol. 40, no. 15, pp. 5575-5592, Oct. 2017.

[22] M. Turner, S. Lenhart, B. Rosenthal, and X. Zhao, "Modeling effective transmission pathways and control of the world's most successful parasite," Theor. Popul. Biol., vol. 86, pp. 50-61, Jun. 2013.

[23] N. E. Mateus-Pinilla, B. Hannon, and R. M. Weigel, "A computer simulation of the prevention of the transmission of Toxoplasma gondii on swine farms using a feline T. gondii vaccine," Prev. Vet. Med., vol. 55, no. 1, pp. 17-36, Sep. 2002.

[24] A. Sullivan, F. Agusto, S. Bewick, C. Su, S. Lenhart, and X. Zhao, "A mathematical model for within-host Toxoplasma gondii invasion dynamics," Math. Biosci. Eng., vol. 9, no. 3, pp. 647-662, 2012.

[25] J. P. Dubey, "Duration of immunity to shedding of Toxoplasma gondii oocysts by cats," J. Parasitol., vol. 81, no. 3, pp. 410-415, Jun. 1995.

[26] J. P. Dubey, D. S. Lindsay, and M. R. Lappin, "Toxoplasmosis and other intestinal coccidial infections in cats and dogs," Vet. Clin. Small Anim. Pract., vol. 39, no. 6, pp. 1009-1034, Nov. 2009.

[27] S. Sultana, G. González-Parra, and A. J. Arenas, “Mathematical modeling of toxoplasmosis in cats with two time delays under environmental effects,” Mathematics, vol. 11, no. 16, p. 3463, Aug. 2023
[28] A. A. Kilbas, I. M. Oleg, and Stefan G. Samko, “Fractional integrals and derivatives (theory and applications).” (1993): 1.
[29] Wang, Ying, and Lishan Liu, “Uniqueness and existence of positive solutions for the fractional integro-differential equation.” Bound. Value Probl., vol. 2017, Art. no. 12, Jan. 2017.
[30] F. Haq, K. Shah, G. Rahman, and M. Shahzad, “Numerical solution of fractional order smoking model via Laplace Adomian decomposition method.” Alex. Eng. J., vol. 57, no. 2, pp. 1061–1069, Jun. 2018.
[31] S. Kumar, A. Kumar, and I. K. Argyros, “A new analysis for the Keller-Segel model of fractional order.” Numer. Algor., vol. 75, no. 1, pp. 213–228, May 2017.
[32] H. Khan, W. F. Alfwzan, R. Latif, J. Alzabut, and R. Thinakaran, “AI-based deep learning of the water cycle system and its effects on climate change.” Fractal Fract., vol. 9, no. 6, p. 361, May 2025.
[33] A. Khan, T. Abdeljawad, and R. Thinakaran, “Computational analysis by artificial intelligence of the fractional-order plant virus spread model.” Fractals, vol. 33, no. 08, pp. 1-21, Jun. 2025.
[34] F. Ali, Z. Shah, N. A. Sheikh, S. Alshehery, I. Khan, and W. S. Koh,“Bioconvection in polar fluid with microstructure: A fractional heat and mass transfer model with non-singular and non-local kernel,” Results Phys., vol. 74, p. 108292, Jul. 2025.
[35] A. Hussain, M. Hammad, A. A. Rahimzai, W. S. Koh, and I. Khan, “Dynamical analysis and soliton solutions of the spacetime fractional Kaup-Boussinesq system,” Partial Differ. Equ. Appl. Math., vol. 14, p. 101205, Jun. 2025.
[36] A. Atangana and D. Baleanu, ”New fractional derivatives with nonlocal and non-singular kernel: theory and application to heat transfer model,” arXiv, preprint: arXiv:1602.03408, Jan. 2016.